Morphogenesis of ellipsoidal camelid red cells: a possible role of a hyperstable membrane skeleton due to a novel alternatively spliced 4.1R

（ラクダ科動物の赤血球が楕円形である仕組み：特徴的構造をもつ 4. 1R による膜骨格の超安定化作用）

Yuqi Chen

Laboratory of Molecular Medicine, Department of Veterinary Clinical Sciences

Graduate School of Veterinary Medicine, Hokkaido University

Contents

Abbreviations

Abbreviations used in this study are as follows:

CBB	Coomassie brilliant blue
CTD	C-terminal domain
F-actin	filamentous actin
GST	glutathione S-transferase
HE	hereditary elliptocytosis
LC-MS/MS	liquid chromatography-tandem mass spectrometry
MBD	membrane binding domain
MCHC	mean corpuscular hemoglobin concentration
MCV	mean corpuscular volume
PBS	phosphate-buffered saline
PCR	polymerase chain reaction
RBCs	red blood cells
SABD	spectrin–actin-binding domain
SDS-PAGE	sodium dodecyl sulfate-polyacrylamide gel electrophoresis
SPR	surface plasmon resonance
V2	variable region 2
aa	amino acid
h4.1R	human 4.1R
hNβSp	N-terminal fragment of human β-spectrin
K_D	equilibrium dissociation constant
k_{ass}	association rate constant
k_{diss}	dissociation rate constant

Preface

Cell shape and function are intrinsically coupled. However, the shapes of red blood cells (RBCs) in vertebrate species are highly diverse, despite these cells sharing a common function in efficient gas exchange in all vertebrates. The RBCs have evolved into two basic shapes; while nucleated nonmammalian RBCs have a biconvex ellipsoidal shape, anuclear mammalian RBCs have a biconcave disk shape. However, the evolutionary molecular mechanism responsible for the difference between ellipsoidal and discoidal shaped RBCs remains unclear.

Intriguingly, camelid RBCs differ in shape from other RBCs. In contrast to other mammalian species, mature RBCs (erythrocytes) of camelid species are flat ellipsoids with markedly reduced membrane deformability in response to applied shear stress. The findings of earlier studies suggest that the membrane skeleton provides the primary molecular basis for the ellipsoid shapes of both camelid and nonmammalian RBCs. The characterization of membrane skeletons in camelid RBCs may therefore enable a determination of the mechanisms that underlie the evolutionary divergence of RBC shapes.

The objective of the present study was to explore the molecular basis for elliptocytic RBC formation in camelids, focusing on the unique protein 4.1R isoform with a molecular mass of 90 kDa ($4.1R^{90}$). Protein 4.1R binds to both spectrin and F-actin through the 10 kDa spectrin–actin-binding domain (SABD) and stabilizes the spectrin–actin membrane skeleton. The analyses were carried out on mRNAs from alpaca reticulocytes and erythroblasts and $4.1R^{90}$ isolated from alpaca RBC membranes. The results showed that alpaca $4.1R^{90}$ contained an additional 19-aa cassette (e14) encoded by alternate exon 14 adjacent to the N-terminal of SABD, that is not included in highly conserved $4.1R^{80}$ proteins in other mammals. Several recombinants of human $4.1R^{80}$ containing alpaca sequences were used to study their ability to form spectrin–actin–4.1R ternary complex by measuring the viscosity of the complexes and also to examine the ability to interact with spectrin. The results showed that the e14 in alpaca

4.1R^{90} markedly enhanced ternary complex formation. The findings of this study suggest that an unusual sequence adjacent to the SABD causes a hyperstabilization of the membrane skeleton with reduced membrane plasticity, leading to the formation of elliptocytic RBCs in camelid species.

The present study has been accepted for publication as described below.

1) Chen, Y., Miyazono, k., Otsuka, Y., Kanamori, M., Yamashita, A., Arashiki, N., Matsumoto, T., Takada, K., Sato, K., Mohandas, N., and Inaba, M. Membrane skeleton hyperstability due to a novel alternatively spliced 4.1R can account for ellipsoidal camelid red cells with decreased deformability. *Journal of Biological Chemistry,* 2023. doi: https://doi.org/10.1016/j.jbc.2023.102877

Introduction

Although cell shape and function are intrinsically coupled, the shapes of red blood cells (RBCs) in vertebrate species are highly diverse, despite these cells sharing a common function in efficient gas exchange in all vertebrates. Vertebrate RBCs have evolved into two basic shapes. All nonmammalian RBCs have a biconvex ellipsoidal shape and are nucleated (Lazarides, 1987; Lazarides and Woods, 1989). Besides the shape, the average RBC size in all camelid species is smaller than most other domestic species with mean corpuscular volumes (MCVs). The mean corpuscular hemoglobin concentration (MCHC) of camelids is generally higher. The size and shape of camelid RBCs facilitate oxygen diffusion by providing a higher effective surface area for gas exchange (Tornquist, 2022). The generation and maintenance of this elliptical shape of nonmammalian RBCs are likely result from co-operative and anisotropic interactions of the plasma membrane-associated membrane skeleton and the transcellular cytoskeleton, involving both intermediate filaments and microtubules (Lazarides, 1987). In contrast, due to the absence of a transcellular cytoskeleton, nucleus, and intracellular organelles, the shape of mammalian RBCs depends exclusively on their plasma membranes, with uniform membrane skeletal structure across the entire surface (Fowler, 2013). The resultant RBCs of most mammalian species have a biconcave disk shape under the hydrostatic conditions and undergo extensive and repeated deformation under shear stress during transit through the microvasculature, resulting in efficient gas and ion transport (Gallagher, 2004; Salomao *et al.*, 2008; Callagher, 2017). However, the evolutionary molecular basis for the difference between ellipsoidal and discoidal shaped of RBCs remains unclear.

Intriguingly, camelid RBCs differ in shape from other RBCs. In contrast to other mammalian species, mature RBCs (erythrocytes) of camelid species are flat ellipsoids with markedly reduced membrane deformability in response to applied shear stress (Smith *et al.*, 1980). Because polychromatophilic RBCs are rounded, camelid RBCs likely acquire their

ellipsoid shape during maturation of reticulocytes into erythrocytes (Andreasen *et al.* 1994), with a circumferential bundle of microtubules, called the marginal band, likely being involved in this transformation of camelid RBCs (Cohen and Terwilliger, 1979). Marginal bands, however, are not required for the maintenance of ellipticity after the cells have fully matured; thus, this filamentous structure is present in reticulocytes but absent in erythrocytes (Cohen and Terwilliger, 1979). The marginal band microtubules, characteristic of all nucleated nonmammalian RBCs (Lazarides, 1987), have also been implicated in the formation of flat discoid shaped avian erythrocytes, with these cells subsequently acquiring an elliptic shape (Barrett and Scheinberg, 1972; Barrett and Dawson, 1974). These findings suggest that the microtubules and membrane skeleton have different roles in flat ellipsoid shape formation, and that the membrane skeleton provides the primary molecular basis for the ellipsoid shapes of both camelid and nonmammalian RBCs. The characterization of membrane skeletons in camelid RBCs may therefore enable a determination of the mechanisms that underlie the evolutionary divergence of RBC shapes.

The membrane skeleton is composed of rod-like $(\alpha\beta)_2$ spectrin tetramers, which are interconnected in a uniform hexagonal lattice through binding to short F-actin at the junctional complex, a process facilitated and stabilized by the protein 4.1R (Ohanian *et al.*, 1984; Mohandas and Gallagher, 2008; Gallagher, 2017). Protein 4.1R binds to both spectrin and F-actin through the 10 kDa spectrin–actin-binding domain (SABD), which in turn is associated with the transmembrane proteins, glycophorin C and band 3, through the N-terminal membrane binding domain (MBD, also designated the FERM domain), connecting the membrane skeleton to the lipid bilayer (Correas *et al.*, 1986; Mohandas and Gallagher, 2008) (Fig. 1). The expression of 4.1R is spatiotemporally regulated by alternative splicing and differential usage of two distinct initiation codons, resulting in the expression of multiple isoforms during terminal erythroid differentiation (Conboy *et al.*, 1991a; Gascard *et al.*, 1998). In late-stage erythroblasts and reticulocytes, the expression of an alternative exon 16, encoding the N-

terminal 21-amino acid (aa) cassette in the SABD, results in the synthesis of the predominant 80 kDa isoform of 4.1R ($4.1R^{80}$) (Conboy *et al.*, 1991b), consisting of a doublet of the polypeptides 80 kDa 4.1Ra and 78 kDa 4.1Rb, in mature RBCs of most mammals (Inaba and Maede, 1988; Inaba *et al.*, 1992). This critical 21-aa cassette is necessary for high-affinity binding to spectrin and actin at the junctional complex, and stabilization of the RBC membrane skeleton (Discher *et al.*, 1993; Discher *et al.*, 1995). Thus, the membrane-associated two-dimensional skeletal network maintains the mechanical stability and integrity of RBCs (Gallagher, 2004; Salomao *et al.*, 2008; Gallagher, 2017). Although the features of several membrane proteins, including spectrin, band 3, and 4.1R, have long been regarded as associated with the elliptic shape of camelid RBCs (Ralston, 1975; Eitan *et al.*, 1976; Khodadad and Weinstein, 1983; Omorphos *et al.*, 1989), the molecular mechanisms associated with the unique morphological features of camelid RBCs and the altered mechanical properties of their membranes remain unclear.

The structural defects of membrane skeletal proteins that weaken or disrupt membrane integrity appear to facilitate a shear stress-induced rearrangement of membrane skeletons, precluding recovery of the biconcave shape, and lead to the formation of permanently deformed RBCs, called elliptocytes (Liu *et al.*, 1990; Liu *et al.*, 1993; Gallagher, 2004; Gallagher, 2017). Various genetic defects of spectrin and 4.1R have been reported to cause hereditary elliptocytosis (HE), in which the degree of hemolytic anemia is dependent on the severity of reduction in the lateral linkages in the membrane skeleton (Gallagher, 2004). Structural defects of 4.1R are much less common than spectrin mutations in HE pathogenesis. However, some 4.1R mutations, including deletion mutations in the SABD associated with moderate anemia (Garbarz *et al.*, 1984; Conboy *et al.*, 1991b; Lorenzo *et al.*, 1994) and intramolecular duplication of SABD associated with a mild phenotype (McGuire *et al.*, 1988; Conboy *et al.*, 1990; Marchesi *et al.*, 1990), have defined the functional significance of the SABD. Camelid 4.1R proteins appears to have a molecular mass higher than the highly conserved $4.1R^{80}$

(Ralston, 1975; Omorphos *et al.*, 1989). It is of interest to determine whether, as in asymptomatic HE due to SABD duplication with a 95 kDa 4.1R mutant ($4.1R^{95}$) (McGuire *et al.*, 1988; Marchesi *et al.*, 1990) , camelid 4.1R has features distinct from other mammalian 4.1R proteins, resulting in rearrangement of membrane skeletal organization following exposure to shear stress in the circulation, and the consequent elliptocytic shape of camelid RBCs.

The objective of the present study was to explore the molecular basis for elliptocytic RBC formation in camelids, focusing on the unique 4.1R isoform with a molecular mass of 90 kDa ($4.1R^{90}$). We first analyzed mRNA from alpaca reticulocytes and examined the amino acid sequence of $4.1R^{90}$ isolated from alpaca RBC membranes. The data showed that alpaca $4.1R^{90}$ contained an additional 19-aa cassette encoded by alternate exon 14 adjacent to the N-terminal of SABD, that is not included in other mammalian $4.1R^{80}$ proteins. A unique amino acid sequence derived from the downstream region of exon 13 was also found in $4.1R^{90}$. Several recombinants of human $4.1R^{80}$ containing alpaca sequences were used to study their ability to form spectrin–actin–4.1R ternary complex (Ohanian *et al.*, 1984) by measuring the viscosity of the complexes and also to examine the ability to interact with β-spectrin (An *et al.*, 2005). The results showed that the exon 14-derived 19-aa cassette (e14) in alpaca $4.1R^{90}$, as well as the duplicated SABDs in human $4.1R^{95}$ mutant (McGuire *et al.*, 1988; Marchesi *et al.*, 1990), markedly enhanced ternary complex formation. The findings of this study suggest that an unusual sequence adjacent to the SABD causes a hyperstabilization of the membrane skeleton with reduced membrane plasticity, leading to the formation of elliptocytic RBCs in camelid species.

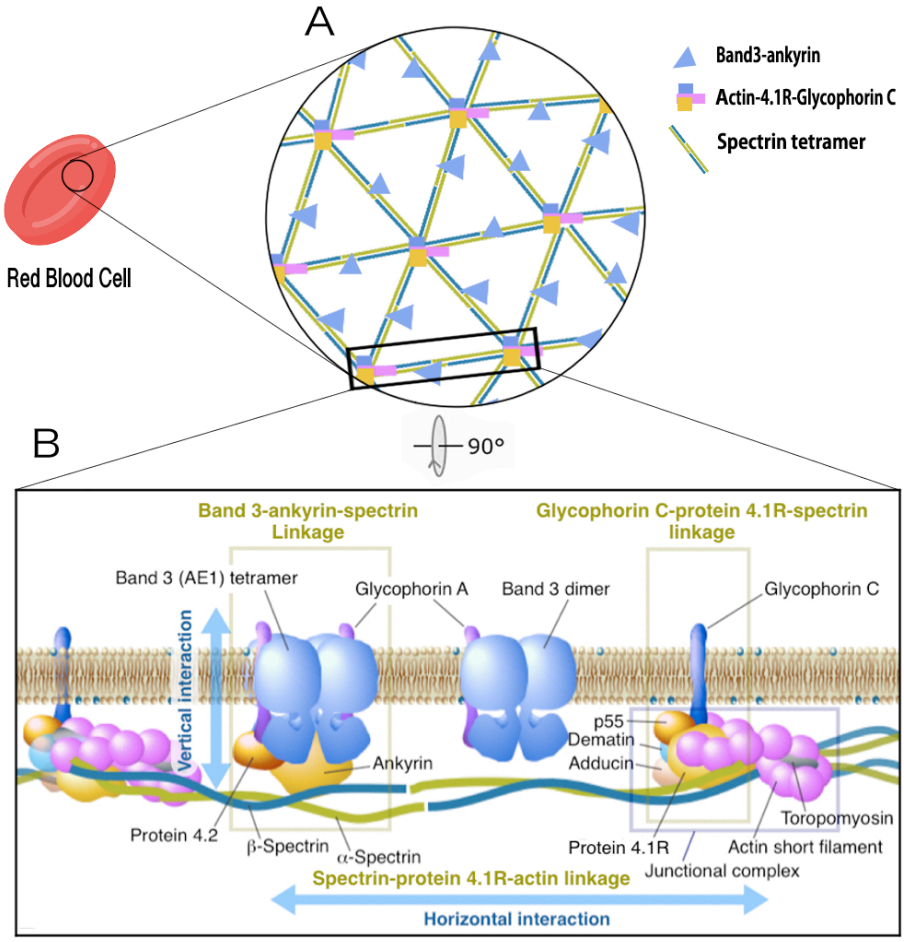

Fig. 1. Overview of the membrane skeleton in RBCs

(A) Basic arrangement of the spectrin–actin membrane skeleton underlying the inner surface of the RBC membrane. (B) Schematic representation of the principal components of the RBC membrane skeleton and its attachments to the plasma membrane through spectrin–ankyrin–band 3 and spectrin–4.1R–glycophorin C linkages (Unsain *et al.*, 2018; Inaba *et al.*, 2022).

Materials and Methods

Animals

Adult male alpacas and dogs were housed at the animal experimentation facility of the Faculty of Veterinary Medicine, Hokkaido University. All experimental procedures were reviewed and approved by the Laboratory Animal Experimentation Committee, Faculty of Veterinary Medicine, Hokkaido University with an approval number 16-0085.

Materials

Antibodies to canine 4.1R, spectrin, and band 3 have been described previously (Inaba and Maede, 1988; Inaba *et al.*, 1996; Komatsu *et al.*, 2010). Rabbit antibody to the exon 14-derived sequence (anti-e14) was generated by injection of a synthetic peptide with the amino acid sequence of NH_2-^{419}Val-Glu-Lys-Thr-His-Ile-Glu-Val-Thr-Val-Pro-Thr-Ser-Asp-Gly-Asp-Gln-Thr-Gln^{437}-COOH. The amino acid sequence encoded by alternative exon 14 is identical in various species, including alpacas, dogs, and humans (Fig. 5). The Asn^{432} residue deduced from the cDNA sequence was converted to Asp (underlined) because Asp was present in the peptides detected by MS/MS analysis (Table 2), presumably due to a rapid post-translational deamidation at the Asn-Gly sequence (Inaba *et al.*, 1992). In some experiments, the aniti-e14 antibody was incubated with an excess amount of alpaca RBC membrane ghosts (200 μg membrane protein/μg antibody) in 10 mM Tris/Cl (pH 7.5), 500 mM NaCl on ice for 2 hours followed by sedimentation of the ghosts by centrifugation. The antibody was subjected to mock treatment by adding it to the ghosts just before centrifugation.

Spectrin tetramers were prepared as reported previously (Ungewickell and Gratzer, 1978; Cohen and Foley, 1980). Briefly, spectrin was extracted from dog RBC membranes and subjected to gel permeation chromatography on a Sepharose 4B column to separate dimers and tetramers. Fractions containing dimers were collected, concentrated by ultrafiltration, and

incubated at 30°C for 2 hours to promote conversion of dimers to tetramers. The samples were again subjected to gel permeation chromatography, and the tetramers were pooled and concentrated. Rabbit muscle actin was purchased from Cytoskeleton Inc.

Analysis of alpaca RBC shapes

The larger and smaller diameters of RBCs were measured on new methylene blue-stained smears of alpaca peripheral blood. RBCs were grouped into younger aggregate reticulocytes, maturing punctate reticulocytes, and erythrocytes. Ellipticity was calculated as (a−b)/a value, where a and b are the larger and smaller diameters, respectively, of RBCs.

The shape of RBC membrane skeletons (Triton shell, the structure formed by erythrocyte membrane protein resistant to solubilization in Triton solution) was examined under light microscopy after solubilization of the membrane in PBS containing 1% Triton X-100 for 30 minutes on ice.

Liquid chromatography (LC)-MS/MS analysis

The amino acid sequence of alpaca RBC 4.1R was determined by Fourier transform-MS/MS as reported previously (Otsu *et al.*, 2013). Briefly, alpaca RBC membrane proteins were separated on 8% SDS-PAGE gels and stained with Coomassie brilliant blue. The gel slices containing 4.1R polypeptides (~90 kDa) were excised and subjected to reduction with 10 mM dithiothreitol, alkylation with 55 mM iodoacetamide, and digestion with 10 μg/ml of trypsin Gold (Promega, Wisconsin, U.S.A.) for 16 hours at 37°C. The tryptic peptides were extracted in 50% acetonitrile/5% trifluoroacetic acid and concentrated by evaporation. The peptides dissolved in 0.1% trifluoroacetic acid were separated and analyzed on a tandemly connected Dionex UltiMate 3000 liquid chromatography system and LTQ Orbitrap Fourier transform-MS/MS system (Thermo Fisher Scientific, Massachusetts, U.S.A.). *De novo* sequencing, comparison with the alpaca reference genome in the NCBI VicPac3.1 database, and post-

translational modification analysis were performed using PEAKS 7 software (Bioinformatics Solutions Inc., Ontario, Canada).

Alpaca erythrocyte 4.1R cDNA

Heparinized blood obtained from alpacas was filtered through an α-cellulose/microcrystalline cellulose column to remove leukocytes and platelets (Inaba and Maede, 1988). mRNA was purified from the resultant RBCs containing reticulocytes, and from erythroblasts amplified from precursor cells in peripheral blood, and was reverse-transcribed into cDNA. Peripheral blood mononuclear cells were cultured in two-phase liquid culture as described (Kiatpakdee *et al.*, 2020). After 6 days in the second phase, the cells (day 6 erythroblasts, consisting mainly of basophilic and polychromatophilic erythroblasts) were harvested, and mRNA was prepared. The 4.1R cDNA fragments were amplified by PCR using the primer pairs Vic41.e4.F and Vic41.e21.R, Vic41.e11.PSYRAA.F and Vic41.e17.KKHHASI.R, or Vic41.e12.TRQASA.F and Vic41.e17.VPEPRP.R (Table 1); cloned; and sequenced. Two independent allelic sequences of cDNAs obtained were deposited in GenBank™ with accession numbers OM890907 and OM890908. The expression of alternative exons in reticulocytes and day 6 erythroblasts was analyzed by PCR using the primers Vic41.5'e13PE.F, Vic41.e17.KKHHASI.R, Vic41.e12.TRQASA.F, and Vic41.seq.e16.R2 (Table 1), followed by direct sequencing and digestion of the amplified cDNA fragments with *Xsp* I or *Taq* I. The relative abundance of cDNA fragments separated by electrophoresis were determined using ImageJ software (National Institute of Health, N.Y.C., U.S.A.).

Plasmids

The plasmids pGST-h4.1R and pGST-βspeN were kindly provided by Shotaro Tanaka, Ichiro Koshino, and Yuichi Takakuwa of Tokyo Women's Medical University (Tokyo, Japan).

pGST-h4.1R contained the wild-type h4.1R cDNA fused to the N-terminal GST in the pGEX-6P-3 (Cytiva, Massachusetts, U.S.A.) backbone. pGST-βspeN contained the GST-fused N-terminal fragment (amino acid residues 1–527) of human β-spectrin in the pGEX-4T-2 (Cytiva, Massachusetts, U.S.A.).

The plasmid for the expression of GST-fused h4.1R lacking SABD (pGST-h4.1ΔSABD) was prepared by inverse PCR of pGST-h4.1R using the primers h41R3'e13.R and h41R5'e18.F (Table 1), followed by ligation. Mutant h4.1R(SABD)2 with duplicated SABD, mimicking the mild HE-causing mutant 4.1[95] (Conboy *et al.*, 1990; Marchesi *et al.*, 1990), was also prepared. The cDNA fragment of exons 16–18 encoding ^{407}Lys–Gln^{529} was amplified from pGST-h4.1R by PCR using the primers h41R5'e16.F and h41R3'e18.R. This fragment was ligated into the vector fragment obtained by inverse PCR of pGST-h4.1R using the primers h41R3'e13.R and h41R5'e16.F; the plasmid pGST-h4.1R(SABD)2 containing duplicated ^{407}Lys–Gln^{529} sequences was also prepared.

To generate h4.1R recombinants containing an alpaca 4.1R-specific PE/e14 sequence, the cDNA fragment was amplified by PCR using the primers Vic41.5'e13PE.F and Vic41.3'e14.R, and ligated into the vector fragment obtained by inverse PCR of pGST-h4.1R with the primers h41prePE.R and h41R5'e16.F. The resultant plasmid pGST-h4.1R[PE14], was used for the expression of the h4.1R recombinant, in which the C-terminal region of the V2 domain (^{391}Asp–Lys^{406}) was replaced by the PE and e14 sequences derived from alpaca 4.1R. The pGST-h4.1R[PE14] was further amplified by inverse PCR with the primers Vic41.3'e13PE.R and Vic41.5'e16.F3, and the proximal ends were ligated to prepare pGST-h4.1R[PE], from which the e14 sequence had been removed.

Preparation of recombinant proteins

Escherichia coli BL21(DE3) pLysS competent cells (Promega, Wisconsin, U.S.A.) were transformed with the appropriate pGEX vectors, and protein expression was induced by

culturing the cells with 1 mM isopropyl-β-thiogalactopyranoside for 6 hours at 30°C. Bacterial cells were collected and lysed in the B-PER reagent (Thermo Fisher Scientific, Massachusetts, U.S.A.). GST-fused h4.1R recombinant proteins in the lysate were trapped on the glutathione Sepharose 4B resin (Cytiva, Massachusetts, U.S.A.) and eluted with 10 mM reduced glutathione.

To measure surface plasmon resonance, some h4.1R recombinants captured on the glutathione Sepharose beads were cleaved from GST by the addition of PreScission protease (Cytiva, Massachusetts, U.S.A.) and eluted from the beads. The proteins were further purified by anion exchange chromatography on a MonoQ column (Cytiva, Massachusetts, U.S.A.) based on the procedure used to purify RBC 4.1R (Inaba and Maede, 1989; Inaba *et al.*, 1992).

The GST-fused N-terminal fragment of human β-spectrin (GST-hNβSp) was generated in BL21(DE3)pLysS cells transformed with pGST-βspeN and purified on a glutathione Sepharose column as described above.

Falling ball viscometry assay

Spectrin–actin–4.1R ternary complex formation was measured by the falling ball viscometry assay, as described (Cohen and Korsgren, 1980; Gimm *et al.*, 2002). In brief, spectrin, F-actin, and GST-h4.1R mutants at appropriate concentrations were mixed in 10 mM Tris/Cl (pH 7.6), 20 mM KCl, 2 mM $MgCl_2$, and 1 mM ATP. A 100 μl microcapillary tube (Drummond Scientific, Pennsylvania, U.S.A.) was filled with this solution, sealed at one end, and incubated at the indicated temperature. After incubation, the tube was placed at a 70° angle from the horizontal; a steel ball (diameter 0.6 mm, Tsubaki-Nakashima Co., Nara, Japan) was placed under the meniscus of the solution using a magnet; and the time required by the ball to fall a specific distance (6 cm) at 25°C was measured. Sedimentation velocity was calculated from the falling time (F_t, s/cm) and converted to apparent viscosity (mPa·s) using glycerol standards of known viscosity. The apparent viscosity of reactions containing only spectrin and

F-actin was used as the control. If the ball did not move from its initial position for 120 seconds, the protein mixture was thought to form a gel. In most measurements, spectrin and F-actin concentrations were 10 and 250 μg/ml, respectively; to this were added GST-h4.1R recombinants at the concentrations of 0–20 μg/ml, yielding a spectrin:actin:4.1R molar ratio of 1:125:0–5.

Binding assay by surface plasmon resonance measurement

Interactions between recombinant h4.1R (h4.1R WT and h4.1R[PE14]) and GST-hNβSp were analyzed by measuring surface plasmon resonance on the Biacore X100 system (Cytiva, Massachusetts, U.S.A.). GST-hNβSp or GST alone as the control, at concentrations of 500 nM, was immobilized on the surface of CM5 sensor chips (Cytiva, Massachusetts, U.S.A.) using an anti-GST antibody (MBL, Nagoya, Japan). Association and dissociation analyses of recombinant proteins at appropriate concentrations (150–1,000 nM) were performed in PBS at 25°C. At the end of each measurement, the chip was regenerated in 10 mM glycine/Cl (pH 2.1). Data were processed with the Biacore X100 evaluation software (Cytiva, Massachusetts, U.S.A.).

Analyses of proteins

RBC membranes were prepared, and SDS-PAGE and immunoblotting were performed, as previously described (Inaba and Maede, 1988, 1989). Protein concentrations were measured and immunofluorescence microscopy performed as described previously (Otsu *et al.*, 2013).

Statistical analysis

All data are expressed as the mean ± S.D. Statistical significance was determined by unpaired Student *t* tests or one-way analysis of variance with Tukey's or Dunnett's multiple comparison test. All statistical analyses were performed by using GraphPad Prism 9.0

(GraphPad), with a *P*-value < 0.05 considered statistically significant.

Table 1. Primers used in the present study

Primers	Nucleotide sequences	Purposes
Vic41.e4.F	5'-GCTTCCCAGAAATCAATCAGA-3'	cDNA cloning
Vic41.e21.R	5'-CAGTCCTCAGAGATTTCGGTCT-3'	cDNA cloning
Vic41.e11.PSYRAA.F	5'-CCCAGTTACCGAGCAGCTAA-3'	cDNA cloning/qPCR
Vic41.e17.KKHHASI.R	5'-TGATGCTGGCATGATGTTTT-3'	cDNA cloning/qPCR
Vic41.e12.TRQASA.F	5'-GACCAGGCAAGCTAGTGCTC-3'	cDNA cloning/qPCR
Vic41.e17.VPEPRP.R	5'-TAGGCCGTGGTTCTGGTACA-3'	cDNA cloning
Vic41.e13.AIAQSEV.F	5'- GCCATTGCTCAGCGTGAGGT-3'	qPCR
Vic41.e17.RPSEWD.R	5'-TTATCCCATTCGCTAGGCCG-3'	qPCR
h41R.3'e13.R	5'-CTTCCATGCTTCTGTGGGCTCTG-3'	Plasmid construction
h41.5'e18.F	5'-CCTCCCCTGGTGAAGACACA-3'	Plasmid construction
h41.5'e16.F	5'-AAAAAGAGAGAAAGACTAGA-3'	Plasmid construction
h41.3'e18.R	5'-CTGGGCAGCCTCATAAGTGA-3'	Plasmid construction
Vic41.5'e13PE.F	5'-GAAGTGCCAGCTGAGCCAG-3'	Plasmid construction/qPCR
Vic41.3'e14.R	5'-CTGTGTTTGGTCACCATTTGA-3'	Plasmid construction
h41.prePE.R	5'-TTCCTTTTTCACTTCAGCCTTCACTGT-3'	Plasmid construction
Vic41.3'e13PE.R	5'-CTTCTCCACTTCTGTGGGCTC-3'	Plasmid construction
Vic41.5'e16.F3	5'-AAAAAGAGAGAAAGACTAGATGGTGAAAAC-3'	Plasmid construction
Vic41seq.e8.F	5'-GTCTTCAACTTCGGCAGGAC-3'	DNA sequencing
Vic41seq.e8.R	5'-TGGGTCATAGTCTCCCAGCT-3'	DNA sequencing
Vic41seq.e10.R	5'-GGCCGAATCTTGATGAAAAA-3'	DNA sequencing
Vic41seq.e14.F	5'-AAAACCCACATCGAGGTCAC-3'	DNA sequencing
Vic41seq.e14.F2	5'-CCTCAAATGGTGACCAAACA-3'	DNA sequencing
Vic41seq.e16.R	5'-AAATCCTCCAACATTAAATTGCT-3'	DNA sequencing/qPCR
Vic41seq.e16.R2	5'-TGTTTTCACCATCTAGTCTCTCTCTC-3'	DNA sequencing/qPCR
Vic41seq.e20.R	5'-GGGTCTCTGAAATTCCACCTT-3'	DNA sequencing
Vic41seq.e21.R	5'-CAGTCCTCAGAGATTTCGGTCT-3'	DNA sequencing

Results

Identification of 4.1R in alpaca RBC membranes

The ellipticity of alpaca erythroid cells increased during the terminal erythroid differentiation, as immature reticulocytes matured into erythrocytes (Fig. 2A), indicating that ellipsoid shape formation is triggered by the mechanical stress-induced membrane structural organization in the circulation as was previously suggested (Andreasen *et al.*,1994). Alpaca RBCs retained their ellipsoid shape following solubilization of the plasma membrane in 1% Triton X-100, suggesting that membrane skeletal organization was irreversibly altered during the formation of elliptic RBCs (Fig. 2B).

As in human RBCs, the predominant component of the major protein 4.1R in the membranes of most mammalian RBCs consists of a doublet of polypeptides ($4.1R^{80}$) (Inaba and Maede, 1988). Immunoblotting analysis showed that the predominant form of 4.1R in alpaca RBC membranes was a doublet of 90 kDa and 88 kDa polypeptides ($4.1R^{90}$), with a size apparently larger than that of $4.1R^{80}$ in other mammalian RBCs (Fig. 2C). A similar $4.1R^{90}$ protein was detected in camel RBC membranes (data not shown), results consistent with previous findings, that the 4.1R protein in camelid RBCs had a higher molecular mass on SDS-PAGE than other mammalian 4.1R proteins (Ralston, 1975; Omorphos *et al.*, 1989). Following solubilization of membranes with Triton X-100, alpaca $4.1R^{90}$ was detected in the insoluble precipitate (Triton shell), along with other membrane skeletal proteins including spectrin and actin (Fig. 2D), indicating that $4.1R^{90}$ participates in the formation and stabilization of the membrane skeleton in alpaca RBCs. Band 3 was not detected in the supernatants of alpaca RBC membranes, consistent with findings on llama RBC membranes (Khodadad and Weinstein, 1983), suggesting that the vast majority of band 3 is principally bound to the membrane skeleton in alpaca RBCs. Although the relative abundance of band 3 was higher in alpaca than human RBC membranes (Fig. 2C) (Eitan *et al*., 1976; Khodadad and Weinstein, 1983), immunoblotting

showed no significant difference in signal intensity between alpaca and human band 3 (Fig. 2D). However, the anti-band 3 antibody used in the present study was raised against band 3 polypeptides purified from dog RBC membranes (Komatsu *et al.*, 2010) and had greater cross-reactivity with human than bovine and alpaca band 3 protein.

Alpaca 4.1R^{90} contains characteristic amino acid sequences derived from exons 13 and 14

Based on the 4.1R sequences in the alpaca genomic DNA sequence database (VicPac3.1), alpaca 4.1^{90} cDNAs prepared from mRNAs of reticulocytes in peripheral blood were cloned and analyzed. The resultant cDNA consisted of exons 4–21, except for exon 15 (Fig. 3). The predicted amino acid sequence of alpaca 4.1^{90} consisted of 652 amino acid residues, 30 amino acid residues larger than human 4.1R^{80} and showed high similarity to the sequence of human 4.1R^{80}. The predicted alpaca 4.1R^{90} sequence contained two peptides adjacent to the SABD but not found in human 4.1R^{80}. The first sequence derived from the region downstream of exon 13, was located at the C-terminus of the V2 region (Conboy, 1999) flanked by the MBD and SABD, and contained many proline (Pro) and glutamic acid (Glu) residues (Figs. 3 and 4A). This Pro- and Glu-rich region, designated the PE region, also showed genotypic variation, with one variation containing three Pro-Ala-Glu and three Pro-Pro-Glu repeats, and the other containing five Pro-Ala-Glu repeats and one Pro-Pro-Glu sequence.

The other sequence characteristic of alpaca 4.1R^{90} was encoded by exon 14, designated e14; this 19-aa peptide was flanked by the PE sequence and the SABD. The amino acid sequence of e14, as well as that of the SABD, was found to be identical or highly conserved among mammalian species (Fig. 5). Amplification of cDNAs encompassing exons 13–17 from alpaca reticulocytes and day 6 erythroblasts generated three distinct fragments, which contained sequences from both exons 14 and 16 (Fig. 4B, *+14/+16*), exon 16 alone (*−14/+16*), or none of these exons (*−14/−16*). The +14/+16 fragment was predominant in both reticulocyte and erythroblast PCR products, with relative abundances of ~75% and ~42%, respectively. No

fragment possessing the sequence from exon 14 but not from 16 was detected. Moreover, PCR amplification of exons 12–16 generated only a 419 bp fragment containing the exon 14-derived sequence from reticulocyte cDNAs (Fig. 4C, *+14*), whereas nearly equivalent amounts of two distinct products, one with (*+14*) and the other without (*−14*) the exon 14-derived sequence, were obtained from erythroblast cDNAs (Fig. 4C). These data demonstrate that exons 14 and 16 are alternatively spliced in alpaca erythroid cells, and that a combination of these exons is expressed in the major 4.1R mRNA species in alpaca erythroblasts and reticulocytes.

MS/MS analysis of SDS-PAGE-purified 4.1R^{90} and a database search detected the amino acid sequences from all the exons comprising 4.1R^{90} cDNA, except that no peptides encoded by exon 19 were detected (Fig. 3 and Table 2), presumably due to the *O*-linked GlcNAc modification of some of the threonine or serine residue(s) in the exon 19-derived region (Inaba and Maede, 1989). The tryptic peptides with the sequences ^{388}Lys-Glu-Glu-…-Glu-Lys^{417} or ^{389}Glu-Glu-…-Glu-Lys^{417} derived from the PE, and the sequence ^{421}Thr-His-…-Gln-Lys^{437} derived from e14, were detected in several independent analyses, demonstrating the involvement of these sequences in alpaca 4.1R^{90}. Immunoblotting of RBC membranes and immunofluorescent staining of RBCs with antibody raised against the e14 cassette further confirmed the unusual expression of the exon 14-derived sequence in alpaca 4.1R^{90} (Figs. 6A and 6B). The anti-e14 antibody detected several minor bands other than 4.1R^{90} in alpaca RBC membranes; some, including the 69/67 kDa doublet, were also recognized by anti-4.1R, whereas others, such as the 59/57 kDa polypeptides, were not. These polypeptides are most likely minor isoforms of 4.1R that contain the e14 cassette but lack other regions, as these bands, as well as the 4.1R^{90} doublet, totally disappeared when the antibody was incubated with excess amounts of leaky ghosts from alpaca RBCs and subsequently used for detection (Fig. 6A, right panel). In contrast, a very low level of e14 cassette expression was detected in a minor isoform of 4.1R in canine RBC membranes (*4.1Ra+/b+* in Fig. 6A), a finding consistent with the very weak expression of exon 14 in late-stage human erythroblasts and reticulocytes (Conboy *et al.*,

1991a; Gascard *et al.*, 1998; Conboy, 1999).

The PE–e14 sequence in alpaca 4.1R^{90} strengthens the membrane skeletal complex formation

To determine if the PE and e14 sequences affect membrane skeletal formation, the effects of these sequences on spectrin–actin–4.1R ternary complex formation were analyzed using the falling ball viscometry assay, employing the GST-fused wild type (WT) of human 4.1R (h4.1R) and h4.1R mutants containing the PE (h4.1R[PE]) or both the PE and e14 (h4.1R[PE14]) sequences (Fig. 7). This analysis also included a mutant h4.1R(SABD)2, which contained the SABD in tandem duplication and mimicked a mild HE-causing mutant 4.1^{95} (Conboy *et al.*, 1990; Marchesi *et al.*, 1990), as well as the h4.1RΔSABD mutant that lacked the SABD. Inclusion of the PE and e14 sequences added a total of 31 amino acid residues, theoretically increasing the molecular mass of 4.1R by approximately 3.5 kDa. However, the molecular masses of GST-fused h4.1R[PE14] and h4.1R(SABD)2 on SDS-PAGE were approximately 10 kDa or 15 kDa larger, respectively, than GST-WT 4.1R^{80}, consistent with the differences between the molecular mass of 4.1R^{80} and the molecular masses of 4.1R^{90} or 4.1R^{95}, respectively (Fig. 7B). The increased negative charge and unordered structure of the PE14 sequence might contribute to the reduced mobility of the protein on SDS-PAGE and the discrepancy between the 3.5 kDa difference in theoretical mass change and the 10 kDa difference in apparent size.

The addition of the WT h4.1R, but not the ΔSABD mutant h4.1R, at increasing concentrations up to 20 μg/ml increased the viscosity of the solution of 10 μg/ml spectrin tetramers and 250 μg/ml F-actin, confirming that the increase in viscosity was induced by spectrin–F-actin–4.1R complex formation through binding of 4.1R to spectrin and actin at the SABD (Figs. 8A–8D). Under the same conditions, h4.1R[PE14] markedly increased viscosity to a level significantly higher than that induced by WT h4.1R. In contrast, the viscosity of

solution containing the h4.1R[PE] mutant did not differ significantly from the viscosity of solution containing WT h4.1R. These findings indicate that the e14 sequence substantially increases the stability of spectrin–actin–4.1R binding at the SABD. In addition, h4.1R(SABD)$_2$ markedly increased ternary complex formation, resulting in about a two-fold higher viscosity than that of the complex formed by h4.1R[PE14]. Furthermore, in the presence of 20 μg/ml spectrin, the addition of the WT h4.1R markedly increased, whereas both h4.1R[PE14] and h4.1R(SABD)$_2$ caused complete gelation of the solution (Fig. 8A).

Compared with WT h4.1R, h4.1R[PE14] had a five-fold lower equilibrium dissociation constant (K_D) for binding to the N-terminal polypeptide of β-spectrin (121 ± 15 nM vs. 633 ± 112 nM, $P < 0.01$, n = 3 each; Fig. 8E). The association rate constant (k_{ass}) of h4.1R[PE14] was significantly higher than that of WT h4.1R ((55.07 ± 8.21) × 10^3 $M^{-1}\cdot s^{-1}$ vs. (5.04 ± 2.16) × 10^3 $M^{-1}\cdot s^{-1}$, $P < 0.001$, n = 3 each; Figs. 8F). the dissociation rate constant (k_{diss}) was higher in h4.1R[PE14] in comparison with the WT (Figs. 8G). These findings account for the higher β-spectrin binding affinity of h4.1R[PE14] than of WT h4.1R.

Table 2. An example of LC-MS/MS data for alpaca 4.1R[90]

An example of database searching for the LC-MS/MS analysis of alpaca 4.1R[90] separated on the SDS-gel. The peptides corresponding to the PE and e14 sequences are highlighted.

Peptide	−10lgP	PTM*
R.SPRPTSAPAIAQSEVTEGSVPGAPVKK.A	70.27	
K.[421]THIEVTVPTSN(+.98)GDQTQK[437].K	67.49	Deamidation (NQ)
R.SM(+15.99)TPAQADLEFLENAK.K	65.25	Oxidation (M)
R.HSNLMLEDLDK.S	63.18	
K.IRPGEQEQYESTIGFK.L	62.94	
K.VSLLDDTVYEC(+57.02)VVEK.H	60.9	Carbamidomethylation
R.SMTPAQADLEFLENAK.K	59.88	
R.SLDGAAVDSADR.S	58.17	
K.TQTVTITDTANAVK.S	58.17	
R.LDGENIYIR.H	57.29	
R.HSNLM(+15.99)LEDLDK.S	54.54	Oxidation (M)
K.[388]KEEVPAEPAEPAEPPEPPEPPEPEPTEVEK[417].V	51.46	
K.NFM(+15.99)ESVPEPR.P	51.25	Oxidation (M)
R.LSTHSPFR.T	51.08	
K.DVPIVHTETK.T	50.54	
K.NFMESVPEPR.P	49.97	
K.VVVHQETEISED	48.06	
R.IVITGDADIDHDQVLVQAIK.E	47.65	
R.QASALIDRPAPH.F	47.02	
R.S(+79.97)LDGAAVDSADR.S	46.97	Phosphorylation (STY)
K.TQTVTITDTAN(+.98)AVK.S	43.64	Deamidation (NQ)
K.HHASISELK.K	42.64	
K.QVHGIPWNFTFNVK.F	42.52	
K.[421]THIEVTVPTSNGDQ(+.98)TQK[437].K	41.58	Deamidation (NQ)
K.KHHASISELKK.N	41.35	
K.TQ(+.98)TVTITDTANAVK.S	39.65	Deamidation (NQ)
K.HHASISELKK.N	39.64	
R.LTSTDTIPK.S	38.83	
K.FLALGSK.F	37.59	
R.QASALIDRPAPHFER.T	36.92	

K.TWLDPAK.E	36.01	
K.RLSTHSPFR.T	35.29	
K.^{389}EEVPAEPAEPAEPPEPPEPPEPEPTEVEK^{417}.V	34.93	
R.INRFPWPK.V	29.63	
R.PTSAPAIAQSEVTEGSVPGAPVKK.A	28.79	
R.SMTPAQAD(+15.99)LEFLENAK.K	28.19	Hydroxylation
R.SPRPTSAPAIAQSEVTEGSVPGAPVK.K	24.31	
K.EQHPDMSVTK.V	23.55	

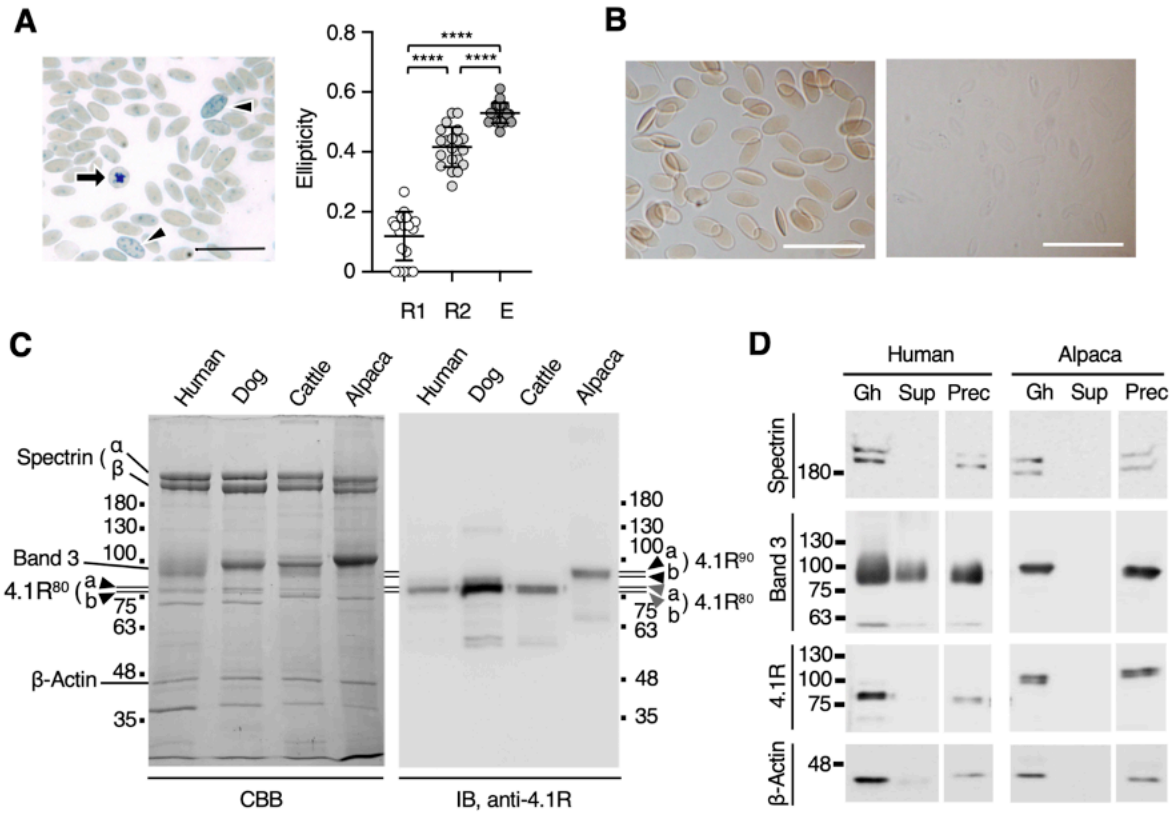

Fig. 2. Characterization of the ellipticity of alpaca RBCs and the 90 kDa 4.1R in alpaca RBC membranes.

A. *Left panel.* A new methylene blue-stained smear of freshly obtained alpaca peripheral blood, showing a younger aggregate reticulocyte (*arrow*) and punctate reticulocytes (*arrowhead*). *Right panel*. Ellipticity of aggregate (*R1*) and punctate (*R2*) reticulocytes and erythrocytes (*E*). Data are expressed as the mean ± S.D. (n = 20). ****$P < 0.0001$ by one-way ANOVA with Tukey's multiple comparison test. Bar, 10 μm. B. Alpaca RBCs washed in PBS (*left*) and ellipsoid Triton shell after solubilization of membranes in PBS containing 1% Triton X-100 on ice for 30 minutes (*right*). Bars, 10 μm. C. 8% SDS-PAGE gel of membrane proteins from human, canine, bovine, and alpaca RBCs stained with Coomassie brilliant blue (*CBB*, 7 μg/lane) and immunoblotted with anti-canine 4.1R antibody (*IB*, 3 μg/lane). The migration of alpaca 4.1R (*4.1R^{90}*, *a* and *b*) was slower than that of human, canine, and bovine 4.1R proteins (*4.1R^{80}*, *a* and *b*). D. Membrane ghosts (*Gh*) from human and alpaca RBCs were incubated in 1% Triton X-100 solution on ice for 1 hour followed by centrifugation at 100,000 × g for 30 minutes to separate the supernatant (*Sup*) and precipitate (*Prec*). Samples equivalent to ghosts containing 2 μg of proteins were subjected to SDS-PAGE and immunoblotting to detect spectrin (*Spectrin*), band 3 (*Band 3*), 4.1R (*4.1R*), and β-actin (*β-Actin*). The migrating positions of size markers are shown in kDa.

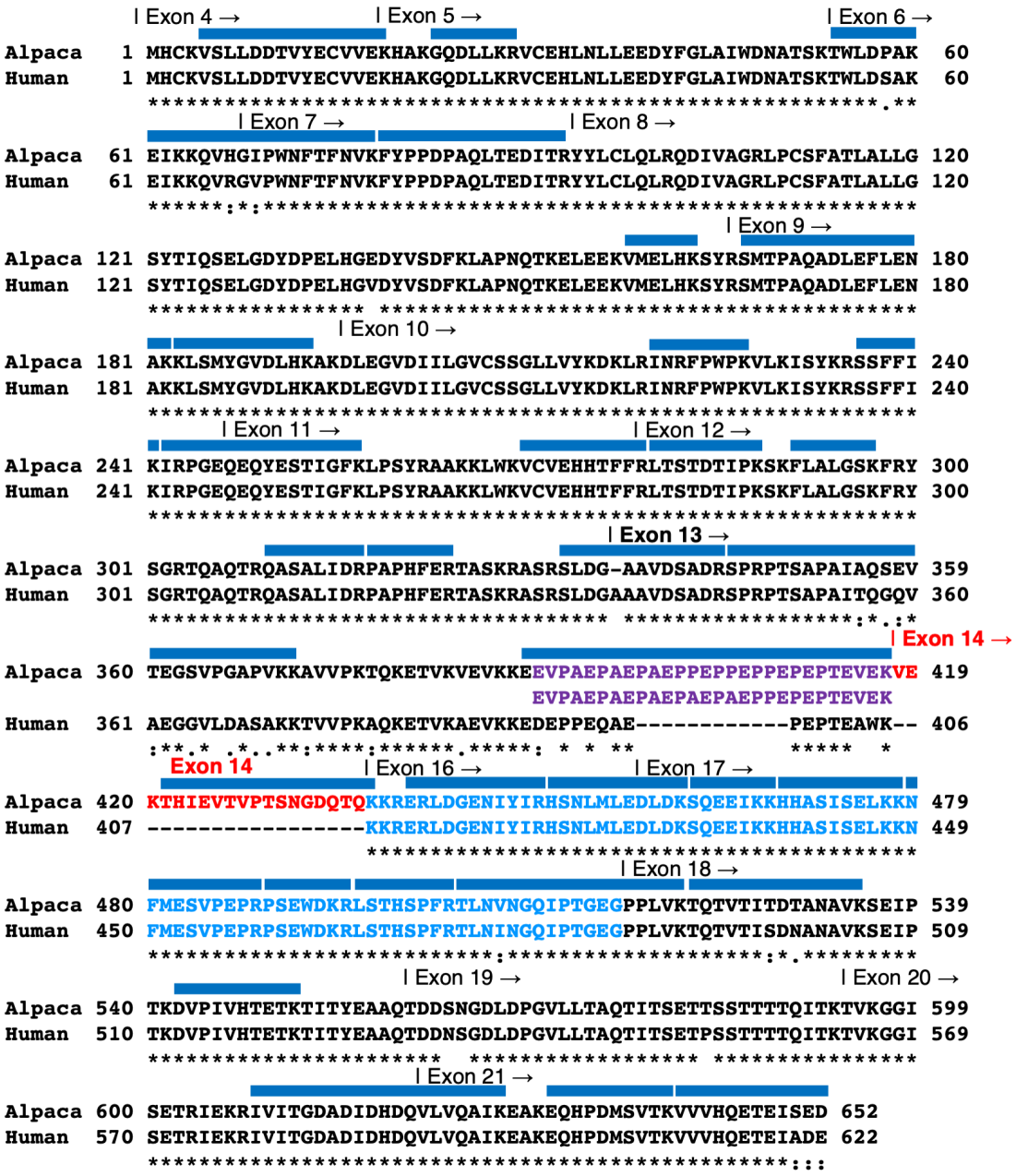

Fig. 3. Comparison of amino acid sequences of alpaca 4.1R^{90} and human 4.1R^{80}. Alignment of the amino acid sequences of the major forms of 4.1R in alpaca (4.1R^{90}) and human (4.1R^{80}) RBCs; asterisks indicate identical amino acid residues. Boundaries for exons are also shown. The alpaca 4.1R^{90} sequence was deduced from its cDNA sequence; the bars in blue above the amino acid residues indicate the peptides detected in LC-MS/MS analysis of the 4.1R^{90} polypeptide separated on SDS-PAGE as described in the text. Purple letters indicate the Pro- and Glu-rich sequence in the C-terminal region of the exon 13-derived sequence ("PE", 28 amino acid residues); red letters indicate the exon 14-derived sequence ("e14", 19 amino acid residues); and blue letters indicate the amino acids in the SABD. The two independent sequences in the PE region were due to allelic differences in nucleotide sequences of exon 13,

one containing three PAE and three PPE repeats (GenBank accession number OM890907) and the other containing five PAE repeats and a single PPE sequence (GenBank accession number OM890908). The human 4.1R sequence is adapted from previous studies (Conboy, 1999; Inaba *et al.*, 1992; Tang *et al.*, 1988).

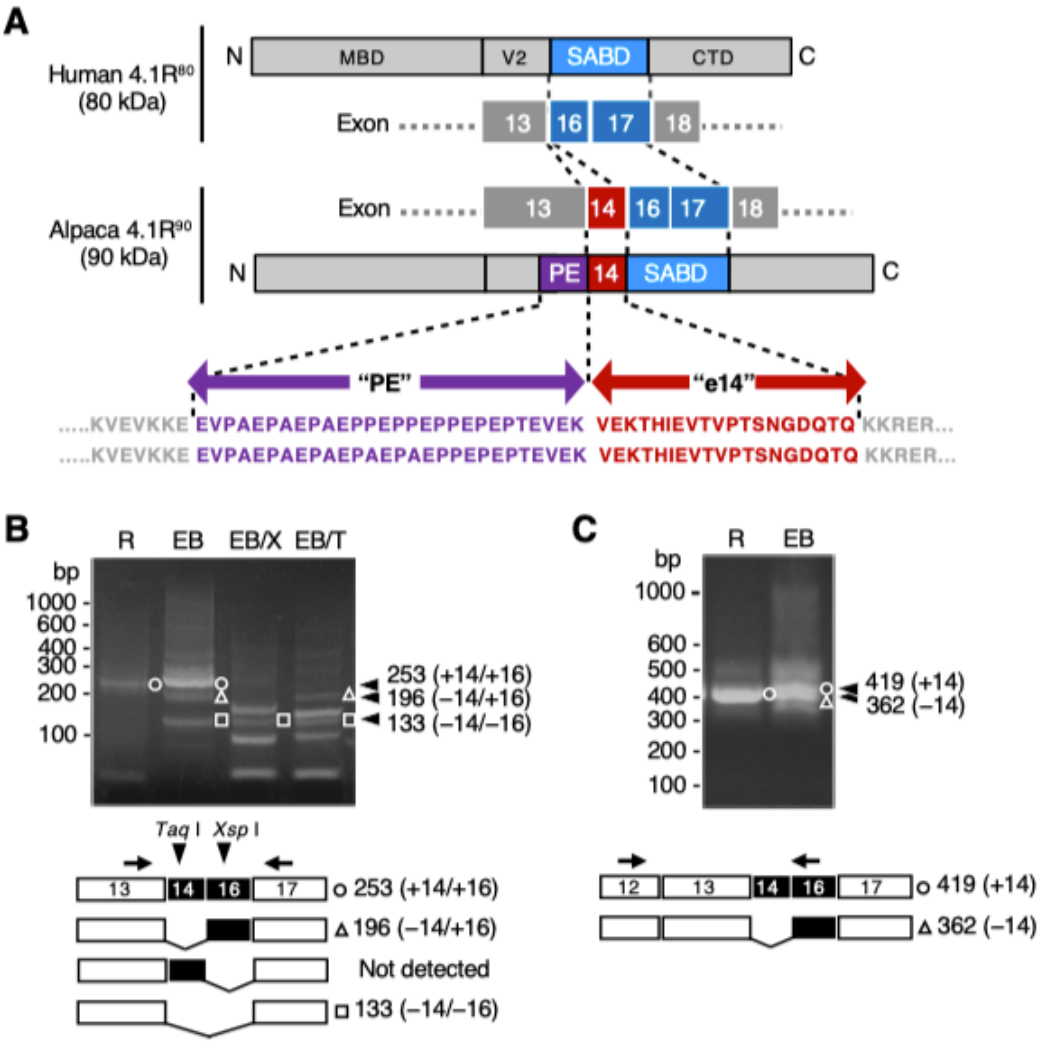

Fig. 4. Involvement of the exon 14-derived sequence in alpaca 4.1R^{90} cDNA

A. cDNA and amino acid sequence analyses of alpaca 4.1R^{90}, focusing on the regions derived from exons 13–17, in comparison with the relevant structures of human 4.1R^{80}. Structural domains of 4.1R^{80} were assigned as described (Inaba and Maede, 1989): MBD, membrane-binding domain; V2, variable region 2; SABD, spectrin–actin-binding domain; and CTD, C-terminal domain. The C-terminal region of V2, which is encoded by exon 13, of alpaca 4.1R^{90} contains a unique amino acid sequence "PE" (shown in purple letters) with two allelic differences. The exon 14-derived sequence "e14" is flanked by the PE and SABD sequences and is shown in red. The complete amino acid sequence and an example of LC-MS/MS analysis of alpaca 4.1R^{90} are shown in the Fig. 3 and Table 2. B. cDNA fragments encompassing exons 13–17 that were PCR amplified from alpaca reticulocyte (*R*) and day 6 erythroblasts (*EB*) using the primers Vic41.5'e13PE.F and Vic41.e17.KKHHASI.R. The arrows show the positions of the primers. The cDNA fragments obtained include a 253 bp fragment containing nucleotides derived from exons 14 and 16 (○, *+14/+16*), a 196 bp fragment with an exon 16 sequence (*Δ*,

−14/+16), and a 133 bp fragment lacking sequences from exons 14 and 16 (□, *−14/−16*). Because exons 14 and 16 contain unique restriction sites for *Taq I* and *Xsp* I, respectively (*arrowheads*), digestion with *Xsp* I (*EB/X*) or *Taq* I (*EB/T*) confirmed that the 253 bp and 196 bp fragments contain exon 14-derived sequence, whereas only 253 bp fragment contains exon 16-derived nucleotides. A cDNA fragment containing exon 14-derived nucleotides alone was not detected. C. cDNA fragments encompassing exons 12–16 PCR amplified from reticulocyte (*R*) and erythroblasts (*EB*) using the primers Vic41.e12.TRQASA.F and Vic41.seq.e16.R2 (*arrows*). The 419 bp fragment containing the exon 14 sequence (○, *+14*) and the 362 bp fragment without this sequence (*⊿, −14*) are indicated.

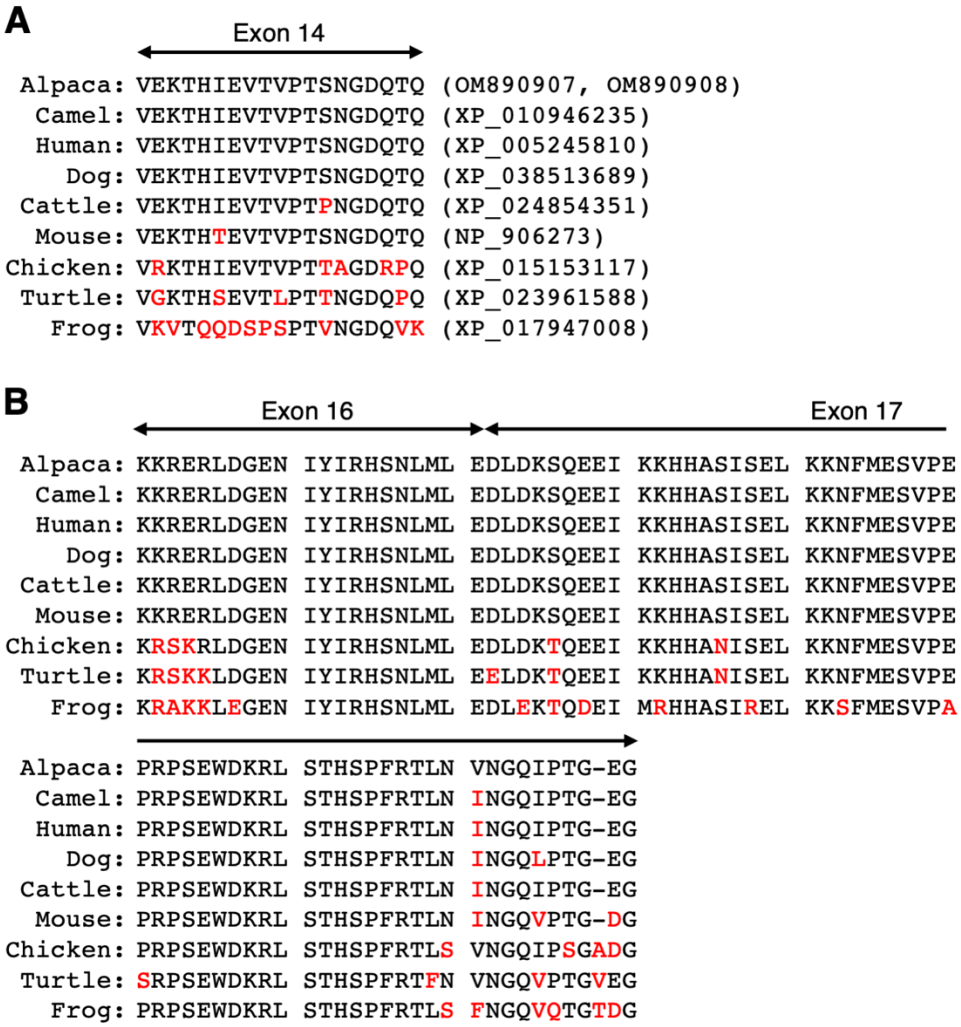

Fig. 5. Alignment of amino acid sequences encoded by the exons 14, 16, and 17.
Alignment of amino acid sequences of e14 (*A*, exon 14) and SABD (*B*, exons 16 and 17) in 4.1R proteins of several species. Amino acid sequences were obtained from the GenBank with accession numbers, alpaca (this study), OM890907 and OM890708; camel, XP_01946235; human, XP_005245810; dog, XP_038513689; cattle, XP_024854351; mouse, XP_906273; chicken, XP_015153117; turtle, XP_023961588; and frog, XP_01794008. Identical amino acid residues are shown in black, whereas different residues are indicated in red.

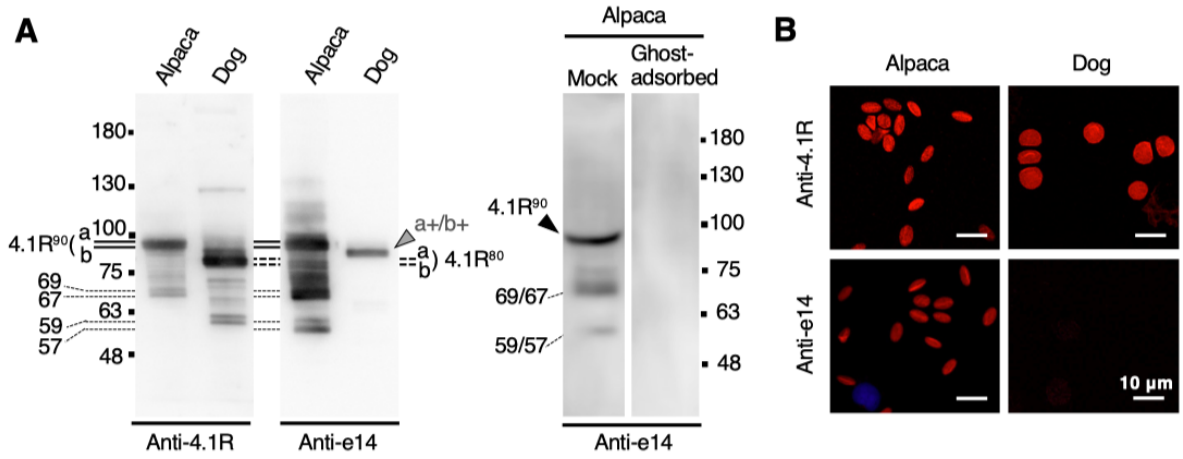

Fig. 6. Immunoblotting and immunofluorescent detection of the exon 14-derived sequence in alpaca 4.1R^{90}.

A. Immunoblotting analysis of 4.1R proteins from alpaca and dog RBC membranes using anti-canine 4.1R (*Anti-4.1R*) and anti-e14 (*Anti-e14*) antibodies. Alpaca 4.1R^{90} reacted with both antibodies, whereas dog 4.1R^{80} reacted only with anti-4.1R antibody. The anti-e14 antibody reacted weakly with proteins slightly larger than 4.1R^{80} (*a+/b+*) in dog membranes, indicating the presence of a 4.1R^{80} isoform having the e14 sequence at a very low level. Each lane contained 3 μg (*alpaca*) and 2 μg (*dog*) membrane proteins (*left panels*). The *right panel* shows the immunoblotting of alpaca RBC membranes with anti-e14 antibody previously incubated with (*Ghost-adsorbed*) or without (*Mock*) an excess amount of alpaca RBC membranes, as described in the Materials and Methods. B. Immunofluorescent detection of 4.1R protein in alpaca and dog RBCs showing the involvement of the e14 sequence in alpaca RBC membranes. Bars, 10 μm.

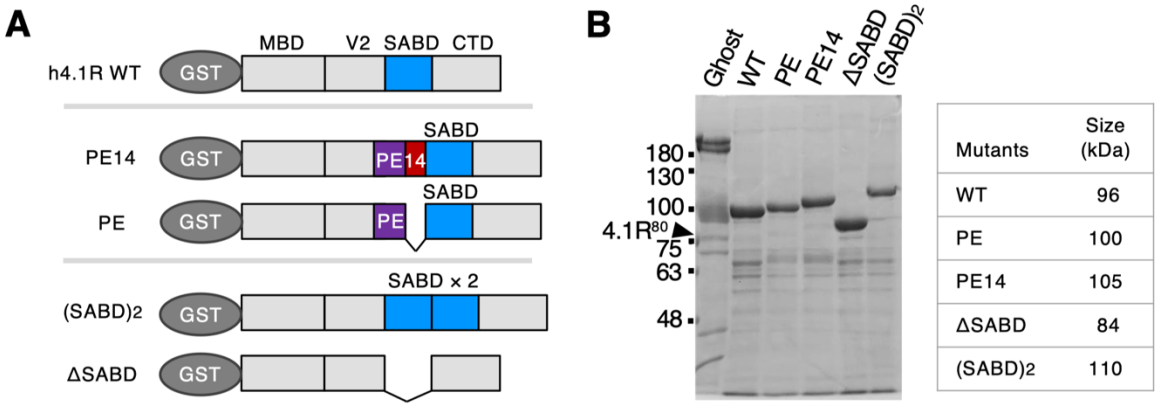

Fig. 7. GST-fused h4.1R mutants used in the gelation assay.

A. Schemes of h4.1R WT and its mutants used in gelation assays. Mutants included *PE14*, h4.1R[PE14]; *PE*, h4.1R[PE]; *(SABD)*$_2$, h4.1R(SABD)$_2$; and *ΔSABD*, h4.1RΔSABD. Assignment of structural domains is described in the legend for Fig. 2. B. Coomassie blue-stained SDS-gel of the purified recombinants. Human RBC membrane proteins are also shown (*Ghost*), with 4.1R^{80} (*4.1R^{80}*) indicated. The apparent molecular masses of GST-fused recombinants and size markers are shown in kDa (*right panel*).

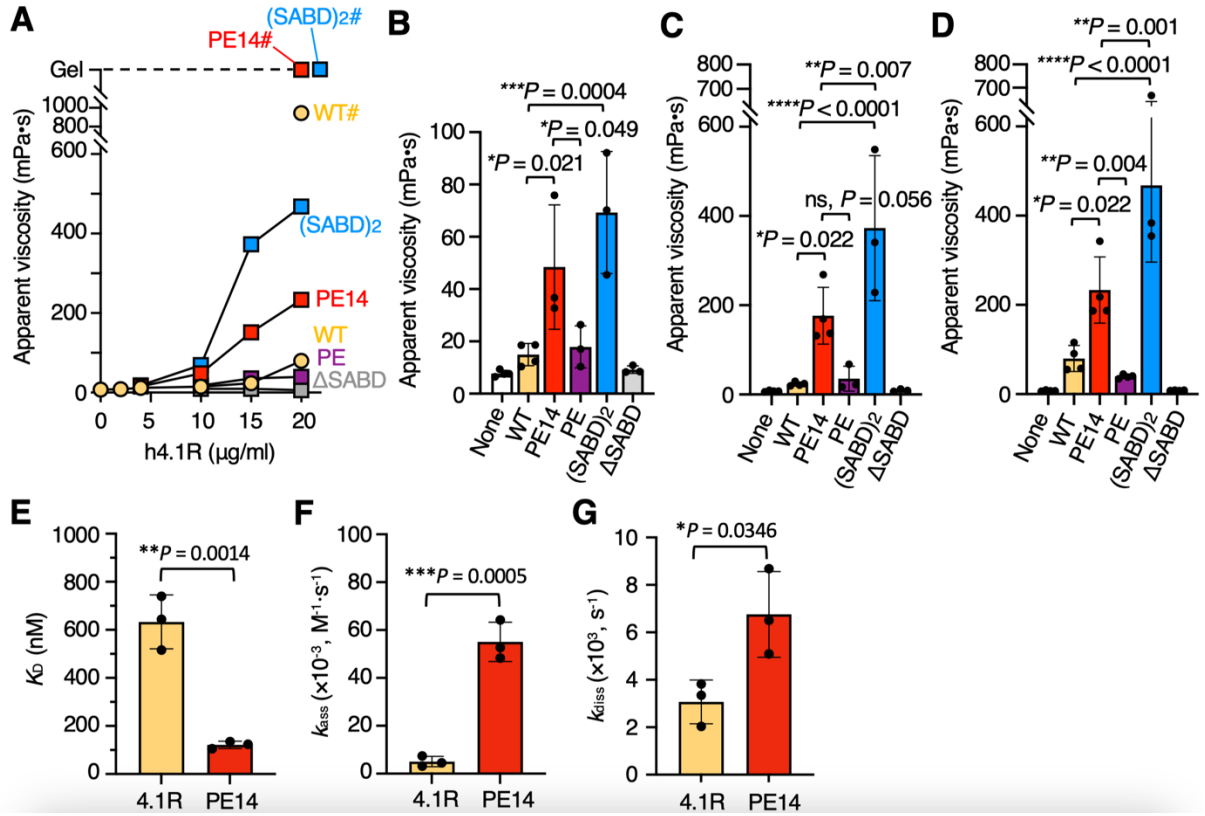

Fig. 8. Effects of the PE14 sequence on spectrin-actin-4.1R ternary complex formation and 4.1R binding to the N-terminal region of β-spectrin.

A. Results of falling ball viscometry assays, showing the apparent viscosity due to the spectrin–actin–4.1R complex formation. Each reaction contained 10 μg/ml spectrin tetramers, 250 μg/ml F-actin, and appropriate concentrations (0–20 μg/ml) of GST-fused h4.1R WT or the h4.1R mutants shown in Fig. 3. Data shown are the means of three independent experiments. The viscosities obtained for the WT (*WT#*) and the PE14 (*PE14#*) and (SABD)$_2$ (*(SABD)$_2$#*) recombinants in the presence of 20 μg/ml spectrin tetramers are also shown. PE14# and (SABD)$_2$# reactions showed complete gelation of the solutions (*Gel*). B–D. Detailed data and comparisons for reactions containing 10 (*B*), 15 (*C*), and 20 μg/ml (*D*) h4.1R recombinants. *None* indicates that the reaction mixture contained only spectrin and F-actin. Data are expressed as the mean ± S.D. (n = 3–4). *P*-values calculated by one-way ANOVA with Dunnett's multiple comparison test. E–G. Results of surface plasmon resonance assays, showing the binding affinities of h4.1R WT (*WT*) and h4.1R[PE14] (*PE14*) to the N-terminal fragment of β-spectrin. K_D values (*E*) calculated from measurements of k_{ass} (*F*) and k_{diss} (*G*). Data are expressed as the mean ± S.D. (n = 3). *P*-values calculated by unpaired *t* tests.

Discussion

The present study showed that camelid 4.1R is unique among RBC 4.1R proteins in that it contains the e14 cassette that is absent from $4.1R^{80}$, the major 4.1R isoform in RBC membranes of other mammalian species. Functionally, the inclusion of e14 markedly increased the formation of the ternary complex of 4.1R, spectrin, and actin through association at the SABD. The gelation activity of SABD in this assay correlated with its ability to strengthen membrane integrity (Discher *et al.*, 1995). Moreover, erythroid-specific expression of the 21-aa cassette from exon 16 has been implicated in the highly efficient interactions of the SABD with spectrin and F-actin necessary to maintain the mechanical stability of RBC membranes, with a reduced yet adequate binding activity being due to the constitutive 59-aa exon 17-coded region alone (Conboy *et al.*, 1991b; Discher *et al.*, 1995). Thus, e14 appears to provide camelid $4.1R^{90}$ the ability to form hyperstable spectrin–actin–4.1R ternary complexes at the junctions in the RBC membrane. Quantification of alternative exon expression indicated that the percentage of the +14/+16 isoform, $4.1R^{90}$, increases as cells mature from erythroblasts to reticulocytes, consistent with a model indicating that this isoform alters membrane properties in mature RBCs.

The membrane skeleton undergoes rearrangement through repeated dissociation and reassociation of spectrin tetramers and dimers, respectively, enabling the RBC membrane to accommodate shear stress-induced distortion in the circulation (Liu *et al.*, 1993; An *et al.*, 2002; Hale *et al.*, 2021). Prolonged membrane skeleton rearrangement with a subsequent deformed configuration precludes the recovery to the biconcave shape and results in the formation of irreversibly deformed RBCs, such as sickled cells and elliptocytes in HE (Liu *et al.*, 1990; Liu *et al.*, 1993; Gallagher, 2004; Gallagher, 2017). In addition, the N-terminal fragment of β-spectrin, containing the binding sites for 4.1R and actin, was shown to be incorporated into junctions in intact membranes, indicating that the ternary complex in the junctions is somewhat

labile (An *et al.*, 2007; Gauthier *et al.*, 2011). The hyperstability of the spectrin–actin–4.1R^{90} interaction suggests the rearrangement of RBC membrane skeletons with reduced plasticity, through the formation of stable junctions, and facilitated the reassociation of spectrin dimers in a deformed configuration, leading to the formation and maintenance of rigid elliptocytes. This scenario can explain the change in shape from sphere to ellipsoid during reticulocyte maturation observed in the present study and the absence of deformative responses of camelid elliptocytes to shear stress (Smith *et al.*, 1980). The present study also showed that the human 4.1R^{95} variant resulting from the SABD duplication mutation was associated with the pathogenesis of HE (Conboy *et al.*, 1990; Marchesi *et al.*, 1990). The markedly increased viscosity of the ternary complex resulting from the addition of h4.1R(SABD)$_2$ strongly suggests that the hyperstable junctions containing the 4.1R^{95} variant bestow increased membrane integrity in this HE subtype (McGuire *et al.*, 1988; Marchesi *et al.*, 1990) , presumably by increasing the number of binding sites for spectrin and actin at the junctions. Thus, camelid 4.1R^{90} and the human 4.1R^{95} variant exemplify membrane-associated proteins whose structural changes result in rigid and hyperstable RBCs, similar to a band 3 mutant in Southeast Asian ovalocytosis (Mohandas *et al.*, 1992; Schofield *et al.*, 1992).

The results of this study also suggest that the e14 cassette increases the binding affinity of 4.1R to β-spectrin, as demonstrated by a surface plasmon resonance measurement assay for the binding of h4.1R mutants to the N-terminal fragment of β-spectrin, suggesting a possible mechanism underlying the increased stability of ternary complex formation. Secondary structure prediction using several algorithms, such as JPred4 (http://www.compbio.dundee.ac.uk/jpred4) and CRNPRED (http://pdbj.org.crnpred), showed that the amino acids derived from exons 13–14, including the PE14 sequence, do not form an appreciably ordered structure. However, e14 may fold upon binding of SABD to its partner proteins spectrin and actin, stabilizing their association. Similar findings have been reported for the functions of several intrinsically disordered proteins, including the N-terminal headpiece of

the erythroid isoform 4.1R^{135} (Nunomura *et al.*, 2011; Wright and Dyson, 2015). These findings, however, are inconsistent with previous results analyzing the interaction of several SABD constructs (Discher *et al.*, 1993). These analyses showed that the N-terminal addition of the e14 sequence to the SABD reduced its affinity to spectrin and F-actin due to steric hindrance (Discher *et al.*, 1993). These discrepancies may be due to differences in the SABD constructs used in these studies, especially the use of whole h4.1R proteins in the present study. Alternatively, the disordered PE sequence confers some role on the effect of e14, although PE itself is unable to form hyperstable ternary complexes.

Hyperstable junctions may also affect the interaction of the membrane skeleton with the lipid bilayer. Band 3 and glycophorin C were each shown to account for 50% of total membrane-bound 4.1R, with the dissociation of 4.1R from band 3 increasing band 3–ankyrin interactions, strengthening the bilayer–skeleton association (An *et al.*, 1996). Notably, K_D values for binding of 4.1R to band 3 and glycophorin C were very similar in the submicromolar (10^{-7} M) range (Nunomura *et al.*, 2009). Therefore, the increased affinity of β-spectrin to 4.1R containing the PE14 sequence may increase the proportion of 4.1R bound to spectrin and actin at the junctions and, by increasing dissociation of 4.1R from band 3, increase the band 3–ankyrin interaction, which has an affinity of 10^{-7}–10^{-8} M (An *et al.*, 1996) , slightly higher than 4.1R–band 3/glycophorin C binding. This hypothesis is consistent with the results of the present study and an earlier study (Khodadad and Weinstein, 1983) showing that most of band 3 in camelid RBC membranes is retained in the precipitate upon solubilization with Triton X-100, presumably because most of band 3 is bound to the membrane skeleton in circulating RBCs. The change in binding partners of band 3 from 4.1R to ankyrin has also been shown to decrease membrane deformability and increase membrane mechanical stability (An *et al.*, 1996), compatible with the properties of camelid RBC membranes.

Decreased membrane deformability could be disadvantageous for animals. However, the size (mean corpuscular volume, MCV) of camelid RBCs ranges from 21–28 fl (Tornquist, 2022)

and is smaller than the RBCs of most other mammals, including humans. The ellipsoid shape and small size may allow camelid RBCs to pass through the microvasculature without significant deformation. However, camelid RBCs are also characterized by their thin and flattened shape and have an average hemoglobin concentration (mean corpuscular hemoglobin concentration, MCHC) higher than that of RBCs in other mammals (Tornquist, 2022). This is consistent with findings showing that high concentrations of hemoglobin restrict the diffusion of CO_2 and HCO_3^- inside RBCs, which is a strong rate-limiting factor for gas turnover (Richardson and Swietach, 2016). Moreover, RBC thickness was found to be reduced as appropriate for their MCHC to compensate for highly restricted cytoplasmic diffusion (Richardson and Swietach, 2016). Earlier studies suggested that morphogenesis of avian RBCs during reticulocyte maturation occurs in two distinct steps, marginal band microtubule-dependent flattening and subsequent ellipsoid formation, by as yet undefined mechanisms (Barrett and Scheinberg, 1972; Barrett and Dawson, 1974). The marginal band is also seen in camelid reticulocytes, but not in erythrocytes (Cohen and Terwilliger, 1979), suggesting that a similar flattening of marginal bands precedes ellipsoid transformation. Therefore, $4.1R^{90}$ likely participates not only in the generation and maintenance of an ellipsoid shape but also in the maintenance of a flattened shape of camelid RBCs, possibly through some intricate three-dimensional interaction of skeletal proteins in equatorial locations. Camelid RBCs are also characterized by their resistance to hypotonic lysis (Perk, 1963; Livne and Kuiper, 1974; Smith *et al.*, 1980) and to dehydration in hypertonic solution without significant shape changes (Yagil *et al.*, 1974; Khodadad and Weinstein, 1983). These properties allow camels to withstand dehydration for extended periods of time and to tolerate rapid ingestion of large volumes of water. The increased band 3 content and protein:lipid ratio on camelid RBC membranes may also be involved in this characteristic osmotic resistance (Levne and Kuiper, 1974; Khodadad and Weinstein, 1983). Hyperstabilization of the membrane skeleton may also contribute to increased osmotic resistance by strengthening the membrane–membrane skeleton association,

as described above.

These findings indicate that the expression of the alternative exon 14 is likely an evolutionary adaptation of camelids to maintain facilitated gas turnover in concert with some genetic traits of RBCs, including MCV and MCHC (Sankaran *et al.*, 2012). The expression of the alternative exon 14 has been found in early erythroblasts in humans, resulting in one of the major isoforms of $4.1R^{135}$, although expression of this exon is decreased and restricted to a very minor population of $4.1R^{80}$ in late erythroblasts and reticulocytes (Conboy *et al.*, 1991a; Gascard *et al.*, 1998). Exon 14 expression is also seen in the brain and endothelial cells (Conboy *et al.*, 1991a; Huang *et al.*, 1993). The functional significance of the exon 14-derived sequence in some 4.1R isoforms is unknown. Because the amino acid sequences encoded by exons 14, 16, and 17 are highly conserved among various mammalian species (Fig. 5), the exon 14 element likely plays some modulatory role in the tissue- and development-specific regulation of skeletal proteins.

In conclusion, the present study described a characteristic feature of camelid $4.1R^{90}$, suggesting the involvement of this protein in elliptocyte formation in camelid species. These findings also indicate that alternative splicing of exons may play a major role in regulating structural organization and membrane function due to the multifunctional skeletal protein 4.1R.

Acknowledgment

I want to express my sincere gratitude to Professor Mutsumi Inaba, Laboratory of Molecular Medicine, Department of Clinical Sciences, Faculty of Veterinary Medicine, Hokkaido University, for his assistance and encouragement while this work.

I also express my gratitude to Professor Kazuhiro Kimura (Laboratory of Biochemistry), Professor Mitsuyoshi Takiguchi (Laboratory of Internal Medicine), and Associate Professor Osamu Ichii (Laboratory of Anatomy), all from Graduate School of Veterinary Medicine, for helpful discussion and critical reading of the manuscript, Dr. Narla Mohandas (New York Blood Center) for his enthusiastic support and critical reading the manuscript, and Dr. Takehisa Matsumoto (Riken BDR) for the effective discussion. I want to acknowledge Associate Professor Kensuke Takada (Laboratory of Molecular Medicine), and all members of the Laboratory of Molecular Medicine for encouragement and technical advice.

Finally, I would like to thank my family, friends, and all those who related for the huge support and encouragement during my Ph.D. life.

Reference

An, X., Debnath, G., Guo, X., Liu, S., Lux, S. E., Baines, A., Gratzer, W., and Mohandas, N. (2005) Identification and functional characterization of protein 4.1 R and actin-binding sites in erythrocyte β spectrin: Regulation of the interactions by phosphatidylinositol-4, 5-bisphosphate. *Biochemistry* **44**, 10681–10688.

An, X., Lecomte, M. C., Chasis, J. A., Mohandas, N., and Gratzer, W. (2002) Shear-response of the spectrin dimer-tetramer equilibrium in the red blood cell membrane. *J. Biol. Chem.* **277**, 31796–31800.

An, X., Salomao, M., Guo, X., Gratzer, W., and Mohandas, N. (2007) Tropomyosin modulates erythrocyte membrane stability. *Blood* **109**, 1284–1288.

An, X.-L., Takakuwa, Y., Nunomura, W., Manno, S., and Mohandas, N. (1996) Modulation of band 3-ankyrin interaction by protein 4.1: functional implications in regulation of erythrocyte membrane mechanical properties. *J. Biol. Chem.* **271**, 33187–33191.

Andreasen, C. B., Gerros, T. C., and Lassen, E. D. (1994) Evaluation of bone marrow cytology and stainable iron content in healthy adult llamas. *Vet. Clin. Pathol.* **23**, 38–42.

Barrett, L. A., and Dawson, R. Ben. (1974) Avian erythrocyte development: microtubules and the formation of the disk shape. *Develop. Biol.* **36**, 72–81.

Barrett, L. A., and Scheinberg, S. L. (1972) The development of avian red cell shape. *J. Exp. Zool.* **182**, 1–13.

Cohen, C. M., and Foley, S. F. (1980) Spectrin-dependent and-independent association of F-actin with the erythrocyte membrane. *J. Cell Biol.* **86**, 694–698.

Cohen, C. M., and Korsgren, C. (1980) Band 4.1 causes spectrin-actin gels to become thixiotropic. *Biochem. Biophys. Res. Commun.* **97**, 1429–1435.

Cohen, W. D., and Terwilliger, N. B. (1979) Marginal bands in camel erythrocytes. *J. Cell Sci* **36**, 97–107.

Conboy, J. (1999) The role of alternative pre-mRNA splicing in regulating the structure and function of skeletal protein 4.1. *Proc. Soc. Exp. Biol. Med.* **220**, 73–78.

Conboy, J. G., Chan, J. Y., Chasis, J. A., Kan, Y. W., and Mohandas, N. (1991a) Tissue-and development-specific alternative RNA splicing regulates expression of multiple isoforms of erythroid membrane protein 4.1. *J. Biol. Chem.* **266**, 8273–8280.

Conboy, J., Marchesi, S., Kim, R., Agre, P., Kan, Y. W., and Mohandas, N. (1990) Molecular analysis of insertion/deletion mutations in protein 4.1 in elliptocytosis. II. Determination of molecular genetic origins of rearrangements. *J. Clin. Invest.* **86**, 524–530.

Conboy, J. G., Shitamoto, R., Parra, M., Winardi, R., Kabra, A., Smith, J., and Mohandas, N. (1991b) Hereditary elliptocytosis due to both qualitative and quantitative defects in membrane skeletal protein 4.1. *Blood* **78**, 2438–2443.

Correas, I., Leto, T. L., Speicher, D. W., and Marchesi, V. T. (1986) Identification of the functional site of erythrocyte protein 4.1 involved in spectrin-actin associations. *J. Biol. Chem*. **261**, 3310–3315.

Discher, D., Parra, M., Conboy, J. G., and Mohandas, N. (1993) Mechanochemistry of the alternatively spliced spectrin-actin binding domain in membrane skeletal protein 4.1. *J. Biol. Chem*. **268**, 7186–7195.

Discher, D. E., Winardi, R., Schischmanoff, P. O., Parra, M., Conboy, J. G., and Mohandas, N. (1995) Mechanochemistry of protein 4.1's spectrin-actin-binding domain: ternary complex interactions, membrane binding, network integration, structural strengthening. *J. Cell Biol.* **130**, 897–907.

Eitan, A., Aloni, B., and Livne, A. (1976) Unique properties of the camel erythrocyte membrane: II. Organization of membrane proteins. *Biochim. Biophys. Acta* **426**, 647–658.

Fowler, V. M. (2013) The human erythrocyte plasma membrane: A Rosetta Stone for decoding membrane–cytoskeleton structure. *Curr. Top. Membr.* pp. 39–88.

Gallagher, P. G. (2004) Hereditary elliptocytosis: spectrin and protein 4.1 R. *Semin. Hematol.* **41** 142–164.

Gallagher, P. G. (2017) Red blood cell membrane disorder. In *Hematology: Basic Principles and Practice*, 7th ed. (Hoffman, R., Benz, E. J., Jr., Silberstein, L. E., Heslop, H. E., Weitz, J. I., Anastasi, J., Salama, M. E., and Abutalib, S. A., eds) Elsevier, Philadelphia, PA.

Garbarz, M., Dhermy, D., Lecomte, M. C., Féo, C., Chaveroche, I., Galand, C., Bournier, O.,

Bertrand, O., and Boivin, P. (1984) A variant of erythrocyte membrane skeletal protein band 4.1 associated with hereditary elliptocytosis. *Blood* **64**, 1006–1015.

Gascard, P., Lee, G., Coulombel, L., Auffray, I., Lum, M., Parra, M., Conboy, J. G., Gascard, P., Lee, G., Coulombel, L., Auffray, I., Lum, M., Parra, M., Conboy, J. G., Mohandas, N., and Chasis, J. A. (1998) Characterization of multiple isoforms of protein 4.1 R expressed during erythroid terminal differentiation. *Blood* **92**, 4404–4414.

Gauthier, E., Guo, X., Mohandas, N., and An, X. (2011) Phosphorylation-dependent perturbations of the 4.1 R-associated multiprotein complex of the erythrocyte membrane. *Biochemistry* **50**, 4561–4567.

Gimm, J. A., An, X., Nunomura, W., and Mohandas, N. (2002) Functional characterization of spectrin-actin-binding domains in 4.1 family of proteins. *Biochemistry* **41**, 7275–7282.

Hale, J., An, X., Guo, X., Gao, E., Papoin, J., Blanc, L., Hillyer, C. D., Gratzer, W., Baines, A., and Mohandas, N. (2021) αI-spectrin represents evolutionary optimization of spectrin for red blood cell deformability. *Biophys. J.* **120**, 3588–3599.

Gallagher, P. G. (2017) Red blood cell membrane disorder. In *Hematology: Basic Principles and Practice*, 7th ed. (Hoffman, R., Benz, E. J., Jr., Silberstein, L. E., Heslop, H. E., Weitz, J. I., Anastasi, J., Salama, M. E., and Abutalib, S. A., eds) Elsevier, Philadelphia, PA.

Huang, J. P., Tang, C. J., Kou, G.-H., Marchesi, V. T., Benz Jr, E. J., and Tang, T. K. (1993) Genomic structure of the locus encoding protein 4.1. Structural basis for complex combinational patterns of tissue-specific alternative RNA splicing. *J. Biol. Chem*. **268**, 3758–3766.

Inaba, M., Gupta, K. C., Kuwabara, M., Takahashi, T., Benz, E. J. Jr., and Maede, Y. (1992) Deamidation of human erythrocyte protein 4.1: possible role in aging. *Blood* **79**, 3355–3361.

Inaba, M., and Maede, Y. (1988) Correlation between protein 4.1 a/4.1 b ratio and erythrocyte life span. *Biochim. Biophys. Acta* **944**, 256–264.

Inaba, M., and Maede, Y. (1989) *O*-*N*-Acetyl-D-glucosamine moiety on discrete peptide of multiple protein 4.1 isoforms regulated by alternative pathways. *J. Biol. Chem*. **264**, 18149–18155.

Inaba, M., and Messick, J. B. (2022) Erythrocyte membrane defects. In Schalm's Veterinary Hematology, 7th ed. (Brooks, M. B., Harr, K. E., Seelig, D. M., Wardrop, K. J., and Weiss, D. J. eds.) pp. 238–247, Wiley-Blackwell, Hoboken, NJ.

Inaba, M., Yawata, A., Koshino, I., Sato, K., Takeuchi, M., Takakuwa, Y., Manno, S., Yawata, Y., Kanzaki, A., Sakai, J., Ban, A., Ono, K., and Maede, Y. (1996) Defective anion transport and marked spherocytosis with membrane instability caused by hereditary total deficiency of red cell band 3 in cattle due to a nonsense mutation. *J. Clin. Invest.* **97**, 1804–1817.

Khodadad, J. K., and Weinstein, R. S. (1983) The band 3-rich membrane of llama erythrocytes: studies on cell shape and the organization of membrane proteins. *J. Membr. Biol.* **72**, 161–171.

Kiatpakdee, B., Sato, K., Otsuka, Y., Arashiki, N., Chen, Y., Tsumita, T., Otsu, W., Yamamoto, A., Kawata, R., Yamazaki, J., Sugimoto, Y., Takada, K., Mohandas, N., and Inaba, M. (2020) Cholesterol-binding protein TSPO2 coordinates maturation and proliferation of terminally differentiating erythroblasts. *J. Biol. Chem*. **295**, 8048–8063.

Komatsu, T., Sato, K., Otsuka, Y., Arashiki, N., Tanaka, K., Tamahara, S., Ono, K., and Inaba, M. (2010) Parallel reductions in stomatin and Na,K-ATPase through the exosomal pathway during reticulocyte maturation in dogs: stomatin as a genotypic and phenotypic marker of high K^+ and low K^+ red cells. *J. Vet. Med. Sci.* **72**, 893–901.

Lazarides, E. (1987) From genes to structural morphogenesis: the genesis and epigenesis of a red blood cell. *Cell* **51**, 345–356.

Lazarides, E., and Woods, C. (1989) Biogenesis of the red blood cell membrane-skeleton and the control of erythroid morphogenesis. *Annu. Rev. Cell Dev. Biol.* **5**, 427–452.

Liu, S.-C., Derick, L. H., Agre, P., and Palek, J. (1990) Alteration of the erythrocyte membrane skeletal ultrastructure in hereditary spherocytosis, hereditary elliptocytosis, and pyropoikilocytosis. *Blood* **76**, 198–205.

Liu, S.-C., Derick, L. H., and Palek, J. (1993) Dependence of the permanent deformation of red blood cell membranes on spectrin dimer-tetramer equilibrium: implication for permanent membrane deformation of irreversibly sickled cells. *Blood* **81**, 522–528.

Lorenzo, F., Dalla Venezia, N., Morle, L., Baklouti, F., Alloisio, N., Ducluzeau, M. T., Roda,

L., Lefrancois, P., and Delaunay, J. (1994) Protein 4.1 deficiency associated with an altered binding to the spectrin-actin complex of the red cell membrane skeleton. *J. Clin. Invest.* **94**, 1651–1656.

Marchesi, S. L., Conboy, J., Agre, P., Letsinger, J. T., Marchesi, V. T., Speicher, D. W., and Mohandas, N. (1990) Molecular analysis of insertion/deletion mutations in protein 4.1 in elliptocytosis. I. Biochemical identification of rearrangements in the spectrin/actin binding domain and functional characterizations. *J. Clin. Invest.* **86**, 516–523.

McGuire, M., Smith, B. L., and Agre, P. (1988) Distinct variants of erythrocyte protein 4.1 inherited in linkage with elliptocytosis and Rh type in three white families. *Blood* **72,** 287–293.

Mohandas, N., and Gallagher, P. G. (2008) Red cell membrane: past, present, and future. *Blood, J. Am. Soc. Hematol.* **112**, 3939–3948.

Mohandas, N., Winardi, R., Knowles, D., Leung, A., Parra, M., George, E., Conboy, J., and Chasis, J. (1992) Molecular basis for membrane rigidity of hereditary ovalocytosis. A novel mechanism involving the cytoplasmic domain of band 3. *J. Clin. Invest.* **89**, 686–692.

Nunomura, W., Gascard, P., and Takakuwa, Y. (2011) Insights into the function of the unstructured N-terminal domain of proteins 4.1R and 4.1G in erythropoiesis. *Int. J. Cell Biol.* **2011**, 943272

Nunomura, W., Parra, M., Hebiguchi, M., Sawada, K.-I., Mohandas, N., and Takakuwa, Y. (2009) Marked difference in membrane-protein-binding properties of the two isoforms of protein 4.1 R expressed at early and late stages of erythroid differentiation. *Biochem. J.* **417**, 141–148.

Ohanian, V., Wolfe, L. C., John, K. M., Pinder, J. C., Lux, S. E., and Gratzer, W. B. (1984) Analysis of the ternary interaction of the red cell membrane skeletal proteins, spectrin, actin, and 4.1. *Biochemistry* **23**, 4416–4420.

Omorphos, S. A., Hawkey, C. M., and Rice-Evans, C. (1989) The elliptocyte: a study of the relationship between cell shape and membrane structure using the camelid erythrocyte as a model. *Comp. Biochem. Physiol.* **94**, 789–795.

Otsu, W., Kurooka, T., Otsuka, Y., Sato, K., and Inaba, M. (2013) A new class of endoplasmic

reticulum export signal ΦXΦXΦ for transmembrane proteins and its selective interaction with Sec24C. *J. Biol. Chem.* **288**, 18521–18532.

Ralston, G. B. (1975) Proteins of the camel erythrocyte membrane. *Biochim. Biophys. Acta* **401**, 83–94.

Richardson, S. L., and Swietach, P. (2016) Red blood cell thickness is evolutionarily constrained by slow, hemoglobin-restricted diffusion in cytoplasm. *Sci. Rep.* **6**, 36018.

Salomao, M., Zhang, X., Yang, Y., Lee, S., Hartwig, J. H., Chasis, J. A., Mohandas, N., and An, X. (2008) Protein 4.1R-dependent multiprotein complex: new insights into the structural organization of the red blood cell membrane. *Proc. Natl. Acad. Sci. USA.* **105**, 8026–8031.

Sankaran, V. G., Ludwig, L. S., Sicinska, E., Xu, J., Bauer, D. E., Eng, J. C., Patterson, H. C., Metcalf, R. A., Natkunam, Y., and Orkin, S. H. (2012) Cyclin D3 coordinates the cell cycle during differentiation to regulate erythrocyte size and number. *Genes Develop.* **26**, 2075–2087.

Schofield, A. E., Tanner, M. J. A., Pinder, J. C., Clough, B., Bayley, P. M., Nash, G. B., Dluzewski, A. R., Reardon, D. M., Cox, T. M., and Wilson, R. J. M. (1992) Basis of unique red cell membrane properties in hereditary ovalocytosis. *J. Mol. Biol.* **223**, 949–958.

Smith, J. E., Mohandas, N., Clark, M. R., Greenquist, A. C., and Shohet, S. B. (1980) Deformability and spectrin properties in three types of elongated red cells. *Am. J. Hematol.* **8**, 1–13.

Tang, T. K., Leto, T. L., Correas, I., Alonso, M. A., Marchesi, V. T., and Benz Jr, E. J. (1988) Selective expression of an erythroid-specific isoform of protein 4.1. *Proc. Natl. Acad. Sci. USA.* **85**, 3713–3717.

Tornquist, S. J. (2022) Hematology of camelids. In *Schalm's Veterinary Hematology,* 7th Ed. (Brooks, M. B., Harr, K. E., Seelig, D. M., Wardrop, K. J., and Weiss, D. J., eds), pp. 1073–1078, Wiley-Blackwell, Hoboken, NJ

Ungewickell, E. and Gratzer, W. (1978) Self-association of human spectrin: a thermodynamic and kinetic study. *Eur. J. Biochem.* **88**, 379–385.

Unsain, N., Stefani, F. D., and Cáceres, A. (2018) The actin/spectrin membrane-associated

periodic skeleton in neurons. *Front. Synaptic Neurosci.* **10**, 10.

Wright, P. E., and Dyson, H. J. (2015) Intrinsically disordered proteins in cellular signalling and regulation. *Nat. Rev. Mol. Cell Biol.* **16**, 18–29.

Abstract

The red blood cells (RBCs) of vertebrates have evolved into two basic shapes, with nucleated nonmammalian RBCs having a biconvex ellipsoidal shape and anuclear mammalian RBCs having a biconcave disk shape. However, the evolutionary molecular mechanism responsible for the difference between ellipsoidal and discoidal shaped RBCs remains unclear. In contrast to other mammalian RBCs, camelid RBCs are flat ellipsoids with reduced membrane deformability, suggesting altered membrane skeletal organization. The characterization of membrane skeletons in camelid RBCs may therefore enable a determination of the mechanisms that underlie the evolutionary divergence of RBC shapes. The present study showed that protein 4.1R, a major component of the membrane skeleton, of alpaca RBCs contains an alternatively spliced exon 14-derived cassette (e14) not observed in the highly conserved 80 kDa 4.1R of other highly deformable biconcave mammalian RBCs. The inclusion of this exon, along with the preceding unordered proline- and glutamic acid-rich peptide (PE), results in a larger and unique 90 kDa camelid 4.1R. Human 4.1R containing e14 and PE, but not PE alone, showed markedly increased ability to form spectrin–actin–4.1R ternary complex in viscosity assays. A similar facilitated ternary complex was formed by human 4.1R possessing a duplication of the spectrin–actin-binding domain, one of the mutations known to cause human hereditary elliptocytosis. The e14- and PE-containing mutant also exhibited an increased binding affinity to β-spectrin compared with wild-type 4.1R. These findings indicate that the presence of 4.1R protein with the e14 cassette results in the formation and maintenance of a hyperstable membrane skeleton, resulting in rigid red ellipsoidal cells in camelid species, and suggest that membrane structure is evolutionarily regulated by alternative splicing of exons in the 4.1R gene.

Abstract in Japanese

脊椎動物の赤血球の形態は大きくふたつに分類できる。哺乳動物を除く脊椎動物の赤血球は有核、両凸面で楕円状であるのに対して、哺乳動物のほとんどは無核で中窪み円盤状の赤血球をもつ。しかし、ガス交換の促進という共通の役割をもつ赤血球が、進化の過程で、なぜ楕円状、円盤状という異なる形態を獲得したのか、また実際に何がそれぞれの形態を規定するのか、それらの分子機作は不明である。興味深いことに、ラクダ科動物の赤血球は他種哺乳動物と異なり、偏平、小球性の楕円形状で膜変形能は極めて低い。細胞骨格や核・細胞内小器官をもたない哺乳動物赤血球では、その形態と変形能はスペクトリン、アクチン、ならびに 4.1R から構成される膜骨格の構造と物理的性状・機能に依存している。したがって、ラクダ科赤血球の楕円形状の要因として、膜骨格が他種哺乳動物とは異なる構造や物理的性状をもつことが示唆される。一方で、膜骨格を構成するタンパク質の異常は、ヒト・動物の遺伝性楕円赤血球症を引き起こす。本研究では、アルパカ赤血球膜骨格のタンパク質 4.1R に焦点をあて、ラクダ科の赤血球が楕円形状をもつ仕組みの解明を目的に、その構造と機能の解析を行った。

哺乳動物赤血球の 4.1R のアミノ酸配列は種間でよく保存されており、その電気泳動上の分子質量は 80 kDa である($4.1R^{80}$)。まず、免疫ブロッティングでの解析で、アルパカ赤血球膜の 4.1R を同定し、これが 90 kDa の質量を示す($4.1R^{90}$)ことを明らかにした。末梢血の網状赤血球から mRNA を調製して 4.1R の cDNA 配列を解析したところ、スペクトリン-アクチン結合ドメイン(SABD)の N 末端側にエクソン 14 由来の配列(e14)が存在することが示された。エクソン 14 は可変スプライシングによって組織・時期特異的に発現するもので、他種の赤血球 $4.1R^{80}$ の mRNA には存在しない。また、エクソン 13 由来配列の C 末端領域にはプロリンとグルタミン酸を多く含む配列(PE)が存在した。赤血球膜から得た $4.1R^{90}$ の LC-MS/MS 解析を行ったところ、e14 と PE に相当する配列が検出された。さらに、抗 e14 抗体を用いた免疫ブロッティングと免疫染色でアルパカ $4.1R^{90}$ が実際に PE と e14 配列をもつことを示した。また、末梢血単核球から 2 段階培養法によって得られた多染性／正染性赤芽球から mRNA を調製してエクソン 14 の発現を網状赤血球と比較したところ、赤芽球の成熟にしたがってエクソン 14 を含む転写産物の割合が大きくなることが示された。

4.1R はスペクトリン、アクチンの両者に結合してスペクトリン-アクチン間結合を安定化させる。ヒト 4.1R (h4.1R WT)に PE と e14 (PE14)を組み込んだ h4.1R[PE14]、あるいは PE を単独で組み込んだ h4.1R[PE]を作製し、スペクトリン-アクチン溶液に

加え、その粘度の変化によって、これらの組換え h4.1R がスペクトリン-アクチン-4.1R 三者複合体の形成に与える影響を解析した。その結果、h4.1R[PE14]はスペクトリン-アクチン-4.1R 三者複合体の形成を著しく促進することが判明した。一方で、h4.1R[PE]には促進作用は認められなかった。また、無症候性のヒト遺伝性楕円赤血球症の原因となる SABD の重複変異体に相当する h4.1R(SABD)$_2$ も h4.1R[PE14]と同様に三者複合体形成を顕著に増強する作用を示した。さらに、β-スペクトリンとの結合において、h4.1R[PE14]は h4.1R WT に比べて平衡解離定数 K_D で５倍高い結合親和性を示した。

これらの知見から、e14 配列をもつ 4.1R^{90} が、スペクトリン-アクチン-4.1R 間結合の増強を介して、末梢循環血中で受けるシアストレスにより伸展・変形した膜骨格構造を不可逆的に超安定化させることが、ラクダ科赤血球の楕円形状の形成と維持の分子基盤であることが明らかになった。本研究の知見は、赤血球形態の多様性が、進化にともなう 4.1R 遺伝子の可変スプライシングによって制御され得ることを示唆するものである。